Copy No. _____

Defence Research and Development Canada
Recherche et développement pour la défense Canada

DEFENCE R&D DÉFENSE

Modelling Assisted Design And Synthesis Of Highly Porous Materials For Chemical Adsorbents

Dr George Shimizu
Department of Chemistry
University of Calgary
Calgary, AB T2N 1N4

PWGSC Contract Number: W7707-042697
Contract Scientific Authority: Paul Saville, 250-363-2892

Defence R&D Canada – Atlantic

Contract Report
DRDC Atlantic CR 2010-201
October 2010

Canada

This page intentionally left blank.

Modelling Assisted Design And Synthesis Of Highly Porous Materials For Chemical Adsorbents

Dr George Shimizu
Department of Chemistry
University of Calgary
Calgary, AB T2N 1N4

PWGSC Contract Number: W7707-042697
CSA: Paul Saville, 250-363-2892

Defence R&D Canada – Atlantic

Contract Report
DRDC Atlantic CR 2010-201
October 2010

Original signed by Paul Saville

Paul Saville

Scientific Authority

Approved by

Original signed by Dr Terry Foster

Dr Terry Foster

Head Dockyard Laboratory Pacific

Approved for release by

Original signed by Ron Kuwahara for

Dr Calvin Hyatt

Head Document Review Panel

Abstract

A new family of metal organic framework materials was studied which relied on organophosphonate molecules as organic linkers between metal ion aggregates as connecting nodes. These materials could form new porous sorbents with the ability to tune the pore size, pore shape and the nature of the chemical functionalities lining the pores. Linear, trigonal and tetrahedral polyphosphonate molecules were studied as well as functionalized linear linkers, all of which were successful in producing new porous solids. Additionally, the use of a linear phosphonate mono ester as a linker was studied, the first use of such a compound in a metal organic framework. New organic linkers were characterized by ^{1}H, ^{13}C and ^{31}P NMR spectroscopy as well as IR spectroscopy and elemental analyses. New network solids were characterized by powder and, when possible, single crystal X-ray diffraction as well as thermogravimetric analysis and gas sorption analyses. Several new families of new porous materials were developed which show promise for sorption of gaseous analytes.

Résumé

Une nouvelle famille de réseaux métallo-organiques a été étudiée et dans laquelle des molécules d'organophosphonate constituent des liens organiques entre les agrégats d'ions métalliques faisant office de noeuds connecteurs. Ces matériaux pourraient former de nouveaux adsorbants poreux offrant la possibilité d'ajuster la taille et la forme des pores, et la nature des fonctionnalités chimiques à la surface des pores. Des molécules de polyphosphonate linéaires, trigonales et tétraédriques ont été étudiées, ainsi que des liens linéaires fonctionnalisés, et toutes ces molécules ont permis de produire de nouveaux solides poreux. En outre, l'utilisation d'un monoester de phosphonate linéaire comme lien a été étudiée, et il s'agissait de la première utilisation d'un tel composé dans un réseau métallo-organique. Les nouveaux liens ont été caractérisés par spectroscopie RMN ^{1}H, ^{13}C et ^{31}P, par spectroscopie infrarouge et par analyse élémentaire. Les nouveaux solides à structure de réseau ont été caractérisés par diffraction de poudre et, si possible, par diffraction des rayons X par cristal unique, analyse thermogravimétrique et analyse d'adsorption de gaz. Plusieurs nouvelles familles de nouveaux matériaux poreux ont été mises au point, et elles sont prometteuses pour la sorption des substances gazeuses à analyser.

This page intentionally left blank.

Executive summary

Modelling Assisted Design And Synthesis Of Highly Porous Materials For Chemical Adsorbents

George Shimizu; DRDC Atlantic CR 2010-201; Defence R&D Canada – Atlantic; October 2010.

Introduction: The ability to tailor the size, shape and chemical nature of pores in a solid is fundamental to controlling the sorption phenomena exhibited by that material. Metal organic frameworks (MOFs) are a relatively new class of porous solids composed of metal ions or metal ion clusters linked by organic spacers that bind to the metals. One of the hallmark properties of this family of compounds is that they have ordered structures (i.e. crystalline) so that samples may be analyzed by X-ray diffraction techniques and structural information at a molecular level obtained. This is a tremendous asset over materials such as amorphous carbons in terms of rationally designing the materials. This proposal concerned specifically the use of the phosphonate group (RPO_3^{2-}) in the formation of new MOFs. The phosphonate group has primarily been studied with linear organic linkers to form layered solids. The layers have a structure where the metal ions bridge the phosphonates into a robust 2-D sheet and the organic groups protrude to define a hydrophobic region. Typically, these organic groups pack efficiently and any sorption phenomena arise due to intercalation of molecules between the sheets. The present study proposed to prepare new organic linkers that would disfavour this classic motif and form true pores in the material. Phosphonate coordination to metals is very strong and the potential to form robust porous solids was high.

Results: Four different organic spacer units were prepared and frameworks studied with different metal ions under different preparative conditions. With each new linker multiple new porous materials were obtained, at least one of which was characterized by X-ray crystallography to give precise molecular dimensions of the pores. Pores were observed in the X-ray structure but definitive proof came in the form of gas sorption measurements showing surface areas in the rages of 100-500 m^2/g. Pores were probed with N_2 gas at 77K and CO_2 at either 273 or 293K. All new compounds were thoroughly characterized. Details of the specific compounds are provided in the report.

Significance: The porous structure, catalytic activity and ability to react with toxic chemicals means that MOFs may find many applications that are of military significance. Their porosity and ability to organize molecules makes them suitable for gas storage, so that either more gas can be stored at an equivalent pressure, or lower pressure is required to store the same amount of gas. Such technology is an enabler for hydrogen and other gaseous fuels. Their porosity, metal centres and organic chemistry provide scope for the development of high throughput catalysts and toxic chemical adsorbents which can be used for personnel protection in respirator technology or for catalytic decontamination. For the basis of modelling of sorption of specific gaseous analytes, including chemical warfare agents, the compounds prepared show very good promise.

Future plans: Precise atomic coordinates are available for modelling studies of the sorption of the new MOF materials as well as corresponding gas sorption data for nitrogen and carbon dioxide. Promising compounds can be made available in gram-sized quantities for direct

experimentation of their sorption for specific analytes not examined. Future work is best focused on gaseous analytes as, the pore apertures may not be of sufficient size for larger guests.

Sommaire

Modelling Assisted Design And Synthesis Of Highly Porous Materials For Chemical Adsorbents

George Shimizu; DRDC Atlantic CR 2010-201; R & D pour la défense Canada – Atlantique; Octobre 2010.

Introduction ou contexte : La capacité de définir la taille, la forme et la nature chimique des pores dans un solide est fondamentale pour maîtriser les phénomènes de sorption présentés par ce matériau. Les réseaux métallo-organiques (MOF) sont une classe relativement nouvelle de solides poreux composés d'ions métalliques ou de groupes d'ions métalliques reliés par des espaceurs organiques qui se rattachent aux métaux. L'une des propriétés caractéristiques de cette famille de composés est qu'ils ont des structures ordonnées (c.-à-d cristallines), de sorte que les échantillons peuvent être analysés par les techniques de diffraction des rayons X et que l'on peut obtenir de l'information structurelle au niveau moléculaire. C'est un atout énorme par rapport à des matériaux comme les carbones amorphes, en termes de conception rationnelle des matériaux. Cette proposition portait spécifiquement sur l'utilisation du groupe phosphonate (RPO_3^{2-}) dans la formation de nouveaux MOF. Le groupe phosphonate a surtout été étudié avec des liens organiques linéaires pour former des solides stratifiés. Les couches ont une structure dans laquelle les ions métalliques relient les phosphonates en feuilles 2D robustes et les groupes organiques font saillie pour définir une région hydrophobe. Généralement, ces groupes organiques s'empilent de manière efficace et les phénomènes de sorption prennent naissance en raison de l'intercalation de molécules entre les feuilles. La présente étude visait à préparer de nouveaux liens organiques qui entraveraient cette structure classique pour former de véritables pores dans le matériau. La coordination des phosphonate aux métaux est très forte et le potentiel de former des solides poreux robustes était élevé.

Résultats : Quatre espaceurs organiques différents ont été préparés et les réseaux ont été étudiés avec différents ions métalliques dans diverses conditions de préparation. Avec chaque nouveau lien, on a obtenu plusieurs nouveaux matériaux poreux, dont au moins un a été caractérisé par cristallographie aux rayons X pour obtenir les dimensions moléculaires précises des pores. On a observé les pores dans la structure de diffraction, mais la preuve définitive a été fournie par la mesure de la sorption de gaz indiquant une surface active de l'ordre de 100 à 500 m²/g. Les pores ont été sondés avec du N_2 gazeux à 77 K et du CO_2 à 273 ou 293 K. Tous les nouveaux composés ont été complètement caractérisés. La description détaillée des composés spécifiques figure dans le rapport.

Importance : En raison de leur structure poreuse, de leur activité catalytique et de leur capacité de réagir avec des produits chimiques toxiques, les MOF peuvent avoir de nombreuses applications militaires importantes. Vu leur porosité et leur capacité d'organiser les molécules, ils sont appropriés pour le stockage de gaz, de sorte que davantage de gaz peut être stocké à une pression équivalente, ou qu'une pression plus faible est requise pour stocker la même quantité de gaz. Une telle technologie se prête bien à l'utilisation de l'hydrogène ou d'autres gaz comme combustibles. Leur porosité, leurs centres métalliques et leur chimie organique se prêtent bien au développement de catalyseurs à haut débit et d'adsorbants de substances chimiques toxiques, utilisables pour la protection du personnel avec la technologie des appareils respiratoires ou par la

décontamination catalytique. Dans l'optique de la modélisation de la sorption d'analytes gazeux spécifiques, y compris les armes chimiques, les composés préparés semblent très prometteurs.

Perspectives : On dispose des coordonnées atomiques précises pour les études par modélisation de la sorption des nouveaux matériaux MOF, ainsi que leurs données correspondantes sur la sorption de gaz, en l'occurrence pour l'azote et le dioxyde de carbone. Des composés prometteurs peuvent être fabriqués en quantités de l'ordre de quelques grammes pour l'étude directe de leur pouvoir de sorption sur des analytes spécifiques non examinés. Les travaux futurs devraient privilégier les analytes gazeux, car les pores pourraient être de taille insuffisante pour des molécules plus grosses.

Table of contents

List of figures

Acknowledgements

Researchers who contributed to the results presented here are: Ms. Junmei Liang, Mr. Jared M. Taylor, Dr. Ramanathan Vaidhyanathan, Dr. Amir Mahmoudkhani.

This page intentionally left blank.

1 Introduction: Porous Phosphonate Metal Organic Frameworks as Sorbents

Metal phosphates had been studied as layered inorganic solids but evolved into the field of "hybrid inorganic-organic" solids by appending organic groups off the rigid inorganic layers.[1] For phosphonates, there are three points that have likely hindered broader proliferation of their study as Metal Organic Frameworks (MOFs), say relative to carboxylates. The first is the predisposition of simple metal phosphonates to a dense layered motif that, while still offering opportunities for function, makes forming high surface area materials a challenge.[2-4] The second reason is that growth of single crystals with phosphonates is generally more difficult as they often precipitate rapidly as less ordered, insoluble phases. While this does not preclude interesting properties, it does make structural characterization, a hallmark property of MOFs, a challenge. The final point is that, again relative to other more studied ligating groups (e.g. COO-, -py), the coordination chemistry of phosphonates is less predictable owing to more possible ligating modes and three possible states of protonation.

Several tactics exist to generate porosity in a metal-phosphonate system. Within the layered structures, one can replace some phosphonates with a non-pillaring group (e.g. phosphate, phosphite or a small monophosphonate) in order to create some interlayer space.[5] This method was introduced by Dines and coworkers.[6] They prepared a pillared zirconium phosphate/ diphosphonate with rough composition of $Zr(O_3PO(CH_2)_6OPO_3)_{0.5}(O_3P(CH_2)_8PO_3)_{0.5}$ and hydrolyzed the hexamethylene ester moieties to obtain porous materials with high surface areas. The problem with this approach is that substitution is random so, even though a porous phosphonate can be formed, structural characterization and a narrow pore size distribution are challenges. A second approach could broadly be classified as examples where the geometry of the organic core in a polyphosphonate disrupts the layered motif and necessitates an open framework. Early work by Alberti and coworkers concerned zirconium phosphite (3,3',5,5'-tetramethylbiphenyldiphosphonate),[7] where the pillar moiety enforced porosity. The specific surface area as determined from BET analysis was 375 m^2g^{-1}. A third approach would be to employ a second functional group on the ligand to chelate the metal ion and direct the structure away from simple layers. This can result in an open phosphonate framework though often these are heteroleptic structures, with the second ligating group playing a substantial role. These latter two approaches will be discussed in more detail as they are germane to the results herein.

2 A Tetraphosphonate Linker for MOFs

Our first approach to forming pores in metal phosphonates was to employ a large, multidirectional ligand that would completely disfavour the formation of a layered inorganic motif. The ligand, 1,3,5,7-tetrakis(4-phenylphosphonic acid)-adamantane, ADTP, was such a molecule as it possessed four phosphonic acid moieties spaced by rigid phenyl groups from an adamantane core (Figure 1). A number of reports of metal complexes with this ligand have appeared. Neumann et al. reported two papers[8, 9] concerning open, but less ordered, frameworks with Ti^{4+} and V^{3+} and this ligand. No crystal structures were obtained but the Ti sample[8] showed

broad features at 5.8° and 11.2° in the powder x-ray diffraction (PXRD). This, with other supporting data, led to a model being proposed with 22 x 9 Å pores. Gas sorption measurements gave a surface area of 557 m^2/g. Using the same ligand, the same group reported catalytic activity of a mesoporous V framework[9] for aerobic oxidation or benzylic alcohols to aldehydes. We reported the crystal structure of the Cu^{2+} network of the same tetraphosphonate ligand.[10] $[Cu_3(H_3ADTP)(OH)(H_2O)_3]\cdot H_2O\cdot MeOH$, consisting of trigonal trinuclear copper clusters linked by the organic spacer into a diamondoid net.

2.1 Experimental

Synthesis of 1,3,5,7-Tetraphenyladamantane (TPA)

Based on a previously reported synthetic route.[1] 1-Bromoadamantane (46.5 mmol) and tert-butylbromide (91. 9 mmol), and benzene (dry, 100 mL) were placed in a dry 250mL round bottom flask fixed with an N_2 inlet and a bubbler into 10% NaOH. The flask was cooled in an ice bath. $AlCl_3$ (3.75 mmol, anhydrous) was then added. A white precipitate formed immediately upon addition. The solution was removed from the ice bath and left to stir for two hours until it had returned to room temperature. It was then refluxed for 1hr. The solution became creamy and yellow over the course of the reaction. The solution was then cooled to room temperature and poured over acidic ice (150 ml ice, 30 ml 6M HCl). More benzene (100 ml) was added and the mixture was left to stir over night. The aqueous phase was then decanted and ether (200mL) was added to the organic phase precipitating the product. It was then filtered to give a white solid. The solid was purified by a Soxhlet extraction over night with chloroform (13.1 g, 63.9%). Product was insoluble in all solvents tried, except boiling DMSO. IR: 3021 cm^{-1}(w), 2920 cm^{-1}(s), 2850 cm^{-1}(m), 1597 cm^{-1} (w), 1495 cm^{-1}(s), 1443 cm^{-1}(s), 1356 cm^{-1}(m), 1079 cm^{-1}(w), 1031 cm^{-1}(w), 750 cm^{-1}(m, 2 bands), 702 cm^{-1}(s). Elemental analysis found: C: 90.57 H: 7.63 N: -0.06, theoretical: C: 92.68 H: 7.32 N: 0%.

Synthesis of 1,3,5,7-Tetrakis(4-iodophenyl)adamantane (TIPA)

TPA (4.59 mmol) was ground with a mortar and pestle with I_2 (9.89 mmol) to give a light pink powder. The pink solid was transferred to a round bottom with stir bar using $CHCl_3$ (40 ml). [Bis(trifluroacetoxy)-iodo]benzene (9.12 mmol) was added to the dark pink slurry, the flask flushed with N_2 and the reaction left to stir for 6h. The slurry was then filtered leaving a maroon filtrate and a pink/brown solid. The solid was Soxhlet extracted with $CHCl_3$ overnight, and the $CHCl_3$ from the extraction was combined with the $CHCl_3$ solution from the reaction. This solution was then washed with a 5% $NaHSO_3$ solution (200 ml), water (200 ml) and then a saturated NaCl solution (100 ml). The $CHCl_3$ was removed by rotovap to give a beige sticky solid, which was subsequently purified by recrystallization from $CHCl_3$/MeOH (9:1). (2.35g, 54.1%). ^1H NMR ($CDCl_3$): δ 2.03 (s, 12H), δ 7.15 (d, 8H), δ 7.63 ppm (d, 8H). IR: 2927 cm^{-1}(m), 2843cm^{-1}(w), 1485cm^{-1}(s), 1392cm^{-1}(m), 1357cm^{-1}(w), 1181cm^{-1}(w), 1072cm^{-1}(w), 1002cm^{-1}(s), 819cm^{-1}(m), 777cm^{-1}(s). Elemental analysis found: C: 42.15 H: 2.33 N: 0.03 theoretical: C: 43.25 H: 2.99 N: 0.0%

Synthesis of 1,3,5,7-Tetra(p-phenylphosphonic acid diethyl ester)-adamantane (ADTP ester): ADTP ester was synthesized via a variation on a previously reported Michalis-Arbuzov reaction, utilizing microwave irradiation, where a high boiling solvent was used in place of microwave irradiation.[2] TIPA (2.28 mmol) was placed in to a round bottom with $NiCl_2$ anhydrous (20%), diisopropylbenzene (80 ml) and fitted with a condenser and a dropping funnel. $P(OEt)_3$ (3 ml, 16.95 mmol) was placed in to the dropping funnel with diisopropylbenzene (6 ml). The solution was brought to reflux and the $P(OEt)_3$ solution added slowly over 8h, followed by refluxing for 24h. Upon cooling a precipitate formed that was subsequently filtered and washed with ether. (1.9 g, 85%). ^{1}H NMR ($CDCl_3$): δ1.33 (t, 6H), δ2.21 (s, 3H), δ4.13 (m, 4H), δ7.59 (m, 2H), δ7.77 ppm (m, 2H). ^{13}C {^{1}H} NMR ($CDCl_3$): δ17.2, δ39.51, δ46.59, δ62.08, δ125.21, δ128.42, δ132.15, δ152.94ppm. ^{31}P ($CDCl_3$): δ18.64ppm. IR: 2982 cm^{-1}(v), 2902 cm^{-1}(v), 1603 cm^{-1}(v), 1394 cm^{-1}(v), 1248 cm^{-1}(s), 1130 cm^{-1}(m), 1053,1120 cm^{-1}(s, 2 bands), 963 cm^{-1}(s), 797,758 cm^{-1}(m, 2 bands). Elemental analysis found: C: 59.46%, H: 6.34%, N: 0.00% theoretical: C: 60.97%, H:6.34%, N:0.00%. Structure characterized through single crystal X-ray diffraction by slow evaporation of a solution of ADTP ester in chloroform/diisopropyl benzene.

Synthesis of 1,3,5,7-tetrakis(4-phenyl phosphonic acid)-adamantane (H_8ADTP): ADTP ester (1.0 mmol) was placed in a round bottom flask with concentrated HCl (20 ml) and refluxed for 48h. It was then filtered to yield a light beige solid, which was dissolved in MeOH and the insoluble material removed by filtration. The MeOH was then removed by vacuum to give a white solid. (0.62g, 82%). ^{1}H-NMR (MeOH-D4): δ2.20 (s, 3H), δ7.54-δ7.94 ppm (m, 4H). ^{31}P-NMR (MeOH-D4, 3 drops conc. HCl) δ18.01ppm. Solid state ^{31}P-NMR: δ19.1575ppm. IR: 2919 cm^{-1}(v), 2852 cm^{-1}(v), 1604 cm^{-1}(s), 1395 cm^{-1}(v), 1137 cm^{-1}(v, broad), 1003, 927 cm^{-1}(s, broad, 2 bands), 827 cm^{-1}(w), 703 cm^{-1}(s). TGA: 25-350ºC -11.62% observed and -12.45% calculated for loss of $6H_2O$, 350-505ºC -35.96% observed and -37.3% calculated for loss of $(PO_3^{2-})_4$, 350ºC decomposition of ADTP. Single crystals were grown by either slow diffusion of chloroform into a methanolic solution of H_8ADTP to obtain an orthorhombic phase, or slow diffusion of a methanolic solution to obtain a triclinic phase.

Growth of Cu_3(ADTPH_3)OH xH_2O yMeOH

ADTPH_8 (0.053mmol) was dissolved in MeOH (3mL) and mixed with $Cu(ClO_4)_2$ $6H_2O$ (0.219mmol) dissolved in MeOH (3mL) to obtain a clear blue solution. The mixture was then placed in a vial and the vial was placed over 20mL hexanes in a jar which was sealed for slow diffusion of hexanes. Growth of small blue hexagonal crystals occurred after 2 days. IR: 3498 cm^{-1}(w), 1604 cm^{-1}(s), 1397 cm^{-1}(s), 1151 cm^{-1}(w), 704cm^{-1}(s), 567 cm^{-1}(m). Single crystal X-ray data show there are two phases of crystal, a monoclinic phase within the solution, and after removal from solution a trigonal phase is obtained.

2.2 Results and Discussion

The single crystal structure of the doubly interpenetrated diamondoid solid, $[Cu_3(H_3$**ADTP**$)(OH)(H_2O)_3]\cdot H_2O\cdot$MeOH, **1**, is reported where the interpenetration still leaves considerable open void space in the solid. The ligand directs the formation of trimetallic Cu clusters as tetrahedral nodes which, along with the adamantyl ligand, enable the diamondoid

structure. Upon desolvation, the structure contracts to a less ordered, but still structurally related phase. Notably, this desolvated material displays permanent porosity as confirmed by CO_2 sorption analysis giving a surface area of ~200 m^2/g.

The ligand, H_8**ADTP** was prepared and complexed to $Cu(ClO_4)_2 \cdot 6H_2O$ in MeOH to obtain a clear blue solution. Diffusion of hexanes into this solution resulted in the growth of small blue octahedral crystals after 2 days. Single crystal X-ray data showed there existed a monoclinic phase within the solution that, upon removal from solution, rapidly converted to a trigonal phase. Although not immediately obvious from the unit cell parameters, these two solids are virtually identical with respect to their molecular structures and so only the more stable trigonal phase, **1**, will be discussed here.

Compound **1** has a structure based on a diamondoid net as shown in Figure 1(a). The formation of a diamond net requires one set of tetrahedral nodes, as provided by **ADTP**, linked by either linear nodes or a second set of tetrahedral nodes. In the case of **1**, a second tetrahedral node comes in the form of a tricopper cluster shown in Figure 1(b). Interestingly, only three metals are involved but the symmetry of the cluster with respect to the phosphonate ligands is a perfect tetrahedron. The three divalent copper centers form a triangular plane which is capped by a μ^3-phosphonate group (Cu-O21= 1.946(3) Å), bridged on the edges by three μ^2-hydrogen phosphonate groups (Cu-O11= 1.985(5), Cu-O12 = 1.965(5) Å), and capped on the opposite face by a μ^3-OH group (Cu-O1= 2.702(7) Å). Thus, the overall cluster, and therefore the network, is neutral. The geometry at each Cu center is square pyramidal with the bond to the capping hydroxyl group occupying the axial site. An equatorial aquo ligand completes the coordination sphere of each Cu center (Cu-O1W= 2.020(10) Å).

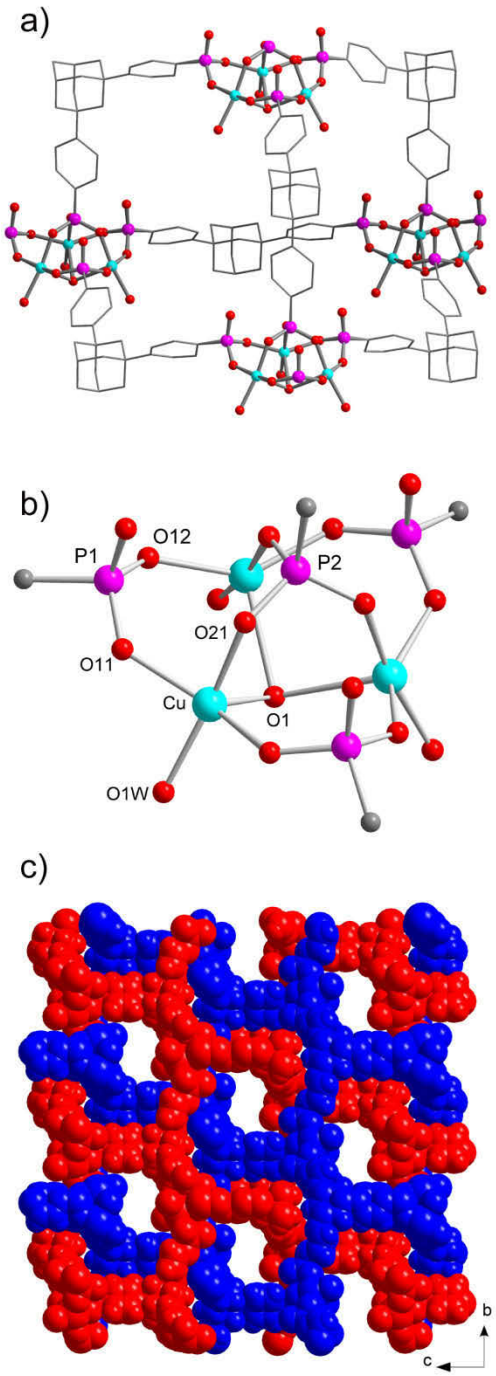

*Figure 1: a) View of a single diamondoid net formed by **1** with truncated molecules of L for clarity. b) Tricopper cluster node with tetrahedrally oriented L molecules. P1 groups are RPO3H- and the P2 group is RPO32-. c) Space-filling rendition of the doubly interpenetrated diamondoid net.*

Diamondoid nets have a topology which readily enables interpenetration to fill potential void space[11] and, in **1**, a two-fold interpenetration is observed. Despite this interpenetration, an open channel structure is still formed as shown in Figure 1(c). Compound **1** has pore entrance widths of 4.1 Å and an oval shaped pore with a minimum width of 8.8 Å and a maximum width of 16.5 Å. Undoubtedly, the additional steric considerations of clusters as nodes prevent higher degrees of interpenetration.[12] The pores are filled by a mixture of disordered water and methanol guest molecules. Additionally, all the phenyl rings of L exhibited rotational disorder. Based on this promising structure, the structural integrity and porosity of the solid were examined.

Combined thermogravimetric analysis/differential scanning calorimetry (TGA/DSC) was performed under both N_2 and air atmospheres in order to determine the stability of the crystals formed. The sample was first allowed to air dry before scanning. The TGA analyses showed an initial mass loss of 13.8% between 25°C and 160°C before an exothermic process of 356kJ/mol (based on a formula unit of $Cu_3(H_3ADTP)OH \cdot 3H_2O$) between 160°C and 235°C where a mass loss of 6.4% occurs, then another continual mass loss of 5.0% before the crystal decomposes at 380°C in air. The exothermic process that occurs between 150°C and 235°C is not quite understood yet, since a structural change does occur upon heating, but this change begins occurring at room temperature and the crystal does not seem to change its crystal structure between 150°C and 240°C since there is no emergence or disappearance of peaks on the powder X-ray pattern. This inference was also tested using VTPXRD in order to monitor and changes in crystallinity in the crystal structure.

The VTPXRD results showed the emergence of a new peak at $2\theta = 6.6°$ even upon heating to 80°C. This peak is attributed to the emergence of a new crystal form upon further desolvation of the crystal under heat. The new peak emerges at a lower 2θ than the original peak at 7.4°, and is consistent with the inference that there is a crystal structure change from monoclinic to trigonal upon desolvation, as the new peak which has emerged matches the simulated PXRD of the trigonal phase. Also, as the sample is heated, the crystal appears to lose much of its long range order, as peak broadening occurs and the diffraction pattern becomes quite noisy, although this may be attributed to the vibrational disorder in the heated sample, and better results would likely be obtained if the sample was allowed to cool and another PXRD was taken of the cooled sample to test for overall crystallinity. Although there is a large exothermic process that occurs between 150°C and 240°C, according to the VTPXRD the sample appears to still be slightly crystalline at 230°C and the peak positions did not deviate significantly from the spectra recorded at 180°C, so the exothermic process is likely not attributed to the crystal structure change.

A surface area measurement was performed on the CuADTP crystal structure using computer simulation with Accelrys MS Modeling. This calculation was performed on the basis that the pores were completely desolvated, and gave a result of about $2800 m^2/g$ as the surface area of the crystal using nitrogen as the adsorbate. This is a good result in comparison to other MOFs. This may show some potential for a high amount of gas adsorption. Also, because the crystal structure is an interpenetrated structure, the number of metal-oxygen bond sites is increased, which may indicate that there is more favourability for a gas molecule to want to adsorb onto the crystal surface. This increased number of metal-oxygen bonds may increase the favorability of the crystal adsorbing gas molecules because it has been shown using inelastic neutron scattering experiments and X-ray diffraction experiments that this is likely the lowest energy site for a gas molecule to be adsorbed on within the MOF crystal structure.

CO_2 sorption analyses were performed on a sample heated to 120°C for 20 hours (Figure 2). A Type 1 isotherm, characteristic of microporous solids, was observed. Dubinin-Radushkevich line fitting gave a surface area of 198 m^2/g and an average pore width of 5.0 Å. These values are comparable to values for smaller pore zeolitic materials and importantly, confirm that there are accessible micropores in **1**. The desorption cycle showed evidence of hysteresis indicating possibly some activation of the solid by CO_2. Given the structure of the Cu cluster involved a bridging hydroxide ion surrounded by three hydrogen phosphonate groups, it seemed plausible that a pathway for the structural distortion would involve elimination of water. A fluoride for hydroxide exchange experiment was conducted where **1** was suspended in a hexanes solution of $(Bu)_4NF$ for two weeks. DSC showed that the resulting solid did not possess the marked exotherm associated with the second mass loss but PXRD showed a similar structural distortion. With solvent alone, the exothermic transition was still observed. CO_2 sorption gave a surface area of 182 m^2/g however, no hysteresis was observed even on a second complete sorption cycle. This observation confirmed that structure was rigid and not being activated. Coupling this result with the PXRD data, it is unlikely that the exchanged solid had a significantly different structure. It did however, retain porosity with the F- exchange serving to rigidify the structure.

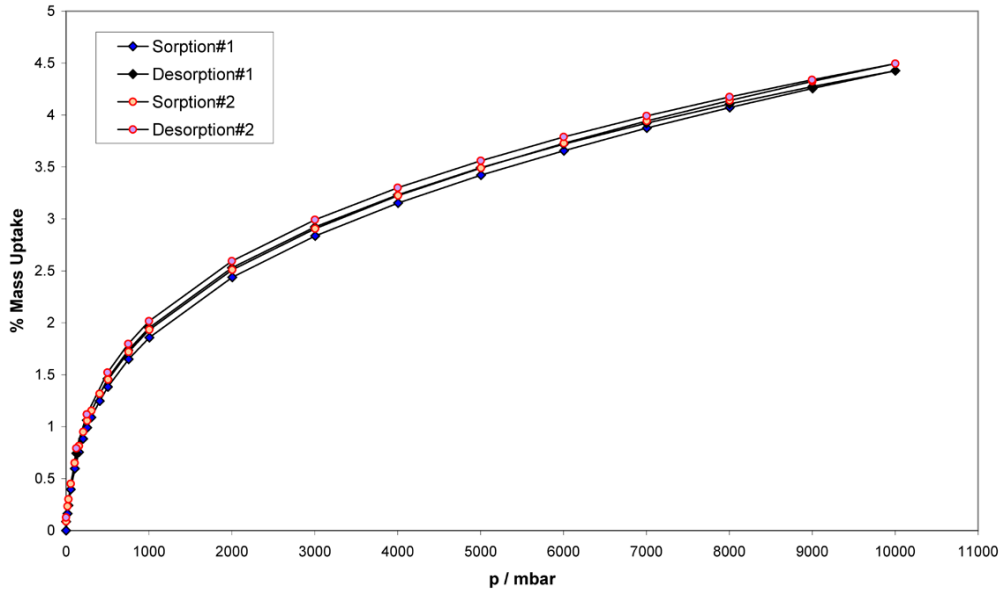

*Figure 2: Two cycles of CO_2 sorption/desorption for F- exchanged **1** showing a Type I isotherm and minimal hysteresis. This correlates to a DR surface area of 182 m^2/g.*

A notable benefit of an approach which would necessarily result in new metal clusters would be that metal clusters/M-O bonds have been cited by several researchers as the primary sites for H_2 adsorption in MOF's. Thus, the coupling of porosity with new oxo clusters could potentially lead to improved H_2 storage materials. In the case of **1**, H_2 storage capacity was measured at 0.24 % by mass which is not a high value. A second intriguing possibility is the potential for magnetic exchange within and/or between clusters leading to porous magnetic solids. Preliminary magnetic measurements on **1** indicate magnetic exchange within the Cu centers of a cluster but of an antiferromagnetic nature. A more complete study will follow along with studies with O_2 as an adsorbing gas. Very recently, two examples of networks with hydroxo-bridged tricopper clusters

and bridging triazolate ligands have been reported.[16] These clusters also show antiferromagnetic exchange.

3 A Triphosphonate Linker for MOFs

We reported the ligand 1,3,5-tris(4-phosphonophenyl)benzene, **PTAB**, a triphosphonate with a rigid D_{3h} geometry.[13] Upon hydrothermal reaction with $Sr(OH)_2$ in the presence of MeOH, the triphosphonate ligand formed a 2-fold interpenetrated, 3-D crystalline solid with the formula, $Sr_2(H_2L)(CH_3OH)(H_2O)_4$, **2**. This compound contained 1-D SrO chains linked together by the trigonal ligand. Each ligand bonded to three different chains and vice-versa, so a three dimensional framework with large 1-D channels resulted.

3.1 Experimental

Synthesis of 1,3,5-tris(4-bromophenyl)benzene

The compound was made by cyclo-trimerization of 4-bromoacetophenone according to the method published elsewhere.[14] In a nominal reaction, 1g of 4-bromoacetophenone was dissolved in 20 mL dry ethanol. Then 1.75 mL $SiCl_4$ was slowly added to the above solution under nitrogen in a flask when kept in a water-ice bath. After 30 min stirring, solution was slowly warmed up to room temperature and kept stirring for 24 h. Then 20 mL distilled water was added to the above reaction to quench it. The product was extracted using dichloromethane (200 mL). The organic layer was separated and dried using $MgSO_4$ and concentrated to 1/3 using a rotary evaporator. Slow evaporation of the remaining solution left pale-yellow crystals of the desired product, which was further purified by recrystallization from $CHCl_3$-Ether to give ~0.7g of the product, yield ~77%. ^{1}H-NMR (Acetone-d6): 7.95s, 7.86s, 7.81s, 7.70s, 7.66s ppm.

Synthesis of 1,3,5-Benzene-tris(phenylphosphonic acid), PTAB

The phosphonate diethylester of PTAB was prepared using a slight modification of the Michaelis-Arbuzov reaction by following a published process.[15] Tris(4-bromophenyl)benzene (1.2 g, 2.2 mmol), anhydrous $NiCl_2$ (28 mg, 0.22 mmol) and 80 mL of 1,3-diisopropylbenzen were added to a 250 mL three neck flask fitted with reflux condenser, N_2 inlet and an addition funnel. The flask was fitted into a regulated heating mantle with magnetic stirring. Triethylphosphite (2.3 ml, 13.2 mmol) and 1,3-diisopropylbenzene (20 mL) were transferred into addition funnel. The system was purged with N_2 for 10 min and kept under static atmosphere of the inert gas. The solution was brought to reflux when triethylphosphite solution was added over a period of 3 hours. The mixture was refluxed for 24 hours and allowed to cool overnight. The resulting dark black solution was vacuum distilled to remove the excess triethylphosphite and the solvent. The product was extracted using 50 mL $CHCl_3$. Removing the solvent by rotary evaporation leaving a yellow oily viscous liquid of the product with 84% yield (1.3 g). Alternatively, the compound was synthesized up to a 50mg quantity under microwave irradiation [8] using the aryl bromide, triethylphosphite and anhydrous $NiCl_2$. Mass EI: m/z (M+H) 715.3(100%), 658.1, 578.4, 529.1,

448.1, 366.2, 241.2, 155.1. ^{31}P-NMR: 19.42 (Methanol-d_4) or 18.48 (Acetone-d_6 or $CDCl_3$) ppm. ^{1}H-NMR (Acetone-d_6): 7.81-8.23 (m, 15H), 4.11 (p, 12H), 1.29 (t, 18H).

Hydrolysis of the diethyl ester using concentrated HCl afforded the corresponding phosphonic acid as a white powder at 90% yield. Solid State CP-MAS ^{31}P NMR: 19.10 ppm. IR (KBr pellet, cm^{-1}): 3398w, br, 2920w, 2146w,br, 1595m, 1489m, 1438w, 1380w, 1143m, 1074m, 1008s, 932m, 887w,sh, 812s, 723m, 677w, 558w, 526w, 483w, 431w. ^{13}C-NMR (Methanol-d_4): 145.22, 145.17, 143.10, 132.89, 132.67, 128.34, 128.19, 126.83.

Synthesis of SrPTAB

SrPTAB can be synthesized as a low-ordered crystalline solid by a reaction of PTAB with $Sr(OH)_2$, $SrCl_2$ or $SrCO_3$. Efforts to crystallize the compound by redissolving it in dilute hydrochloric acid and slow evaporation were unsuccessful. However, crystallinity can be improved by prolong hydrothermal dissolution of the powder at elevated temperatures, as followed by PXRD. By careful examination of variation of reactants ratio, a reaction of $Sr(OH)_2$ with PTAB at 1:1 ration was found to be promising. Crystals of SrPTAB was grown hydrothermally by a reaction of PTAB (200 mg, 0.36 mmol) and $Sr(OH)_2$ (44 mg, 0.36 mmol) in a mixture of distilled water (7 ml) and methanol (3 ml) in a Teflon lined Parr autoclave with the capacity of 23 mL. A temperature program is used as the following: Rising from room temp to 140 °C (30 min), isothermal at 140 °C for 2 days and cooling to room temp during 3 days. Colorless needle crystals were obtained and kept in mother liquor. Crystals turn opaque after 24 hours even sitting in mother liquor and quickly desolvate when removed from solution. IR (KBr pellet, cm^{-1}): 3396s,br, 2339w,sh, 1635w,sh, 1599m, 1556w, 1499w, 1439w, 1383w, 1139m, 1061m, 970m, 899w, 818m, 694m, 574w. Solid State CP-MAS ^{31}P-NMR: 12.86 ppm.

Synthesis of CaPTAB

CaPTAB was prepared using the same method as mention above, but no single crystals were obtained. CaPTAB can be prepared as white crystalline powder in quantitative yield. IR (KBr pellet, cm^{-1}): 3399s,br, 2331w,sh, 1635w,sh, 1599m, 1555w, 1491w, 1435w, 1384w, 1137m, 1061m, 978m, 910w, 820m, 695m, 586w. Solid State CP-MAS ^{31}P NMR: 12.11 ppm.

3.2 Results and Discussion

The ligand **PTAB** was prepared using a slight modification of the Michaelis-Arbuzov reaction by following a published procedure.[15] Sr^{2+} complexes of **L** can be synthesized as a low crystalline solid by a reaction of **L** with $Sr(OH)_2$, $SrCl_2$ or $SrCO_3$. Efforts to crystallize the compound by redissolving it in dilute hydrochloric acid and slow evaporation were unsuccessful. However, crystallinity can be improved by prolonged hydrothermal dissolution of the powder at elevated temperatures, as followed by PXRD. Crystals of Sr(**PTAB**)$(CH_3O)(H_2O)_4$**, 2**, were grown hydrothermally by a reaction of **L** and $Sr(OH)_2$.

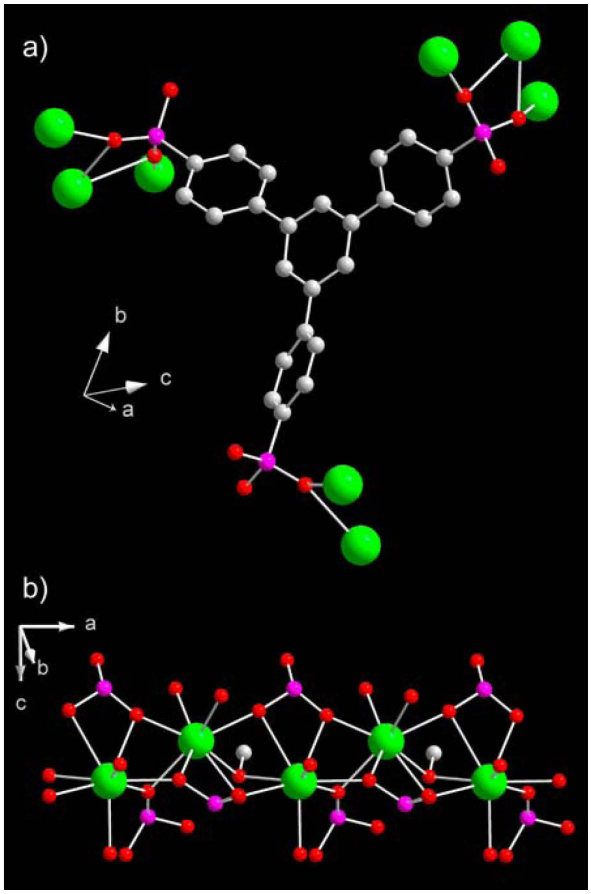

*Figure 3: Building units of **2**, a) the coordination of RPO_3 groups of **PTAB** to the Sr ions; b) the one-dimensional SrO chains formed by the coordination of the phosphonate, methoxy and water to the Sr atoms.*

The three-dimensional structure of **2** is built up from the linking of one dimensional SrO chains by the phosphonate ligand, **PTAB**. The inorganic backbone is composed of face sharing SrO_8 monocapped pentagonal biprisms. The two crystallographically independent Sr centers are coordinated by 5 phosphonate oxygens, a μ_2 bridging methoxy oxygen and two water molecules (Fig. 3). The phosphonate groups of **PTAB** show two different binding modes, while P1 binds only through one oxygen to two different Sr centers, P2 and P3 each bind through two of their oxygens to three different Sr centers. Thus, each ligand connects to three different SrO chains and vice versa. Such connectivities result in a three-dimensional framework with large one-dimensional channels (19.34(1) x 14.83(1)Å) along the *a*-axis (Fig. 4a). Parts of the channels are lined by the hydrophobic phenyl rings of **PTAB**, and the rest by the polar phosphonate groups. From any single 1-D inorganic column, pendant organic groups of **PTAB** are separated by 6.92(1) Å along the *a*-axis, a distance suited to including another aromatic ring. From examination of a single net, the structure appears three-dimensionally porous, however, both the large pores and spacing between aryl units of **PTAB** are sufficient to allow two-fold interpenetration of the structure (Fig. 4b). This interpenetration results in the efficient pi-stacking of the central aryl rings of **PTAB** molecules from different nets (centroid - centroid distance =

3.52(1)Å), which serve to augment the stability of the framework. The two independent nets are offset by 60° so that, while the central aryl rings of **PTAB** are pi-stacked, clefts remain between the three peripheral aryl rings (Fig. 4b).

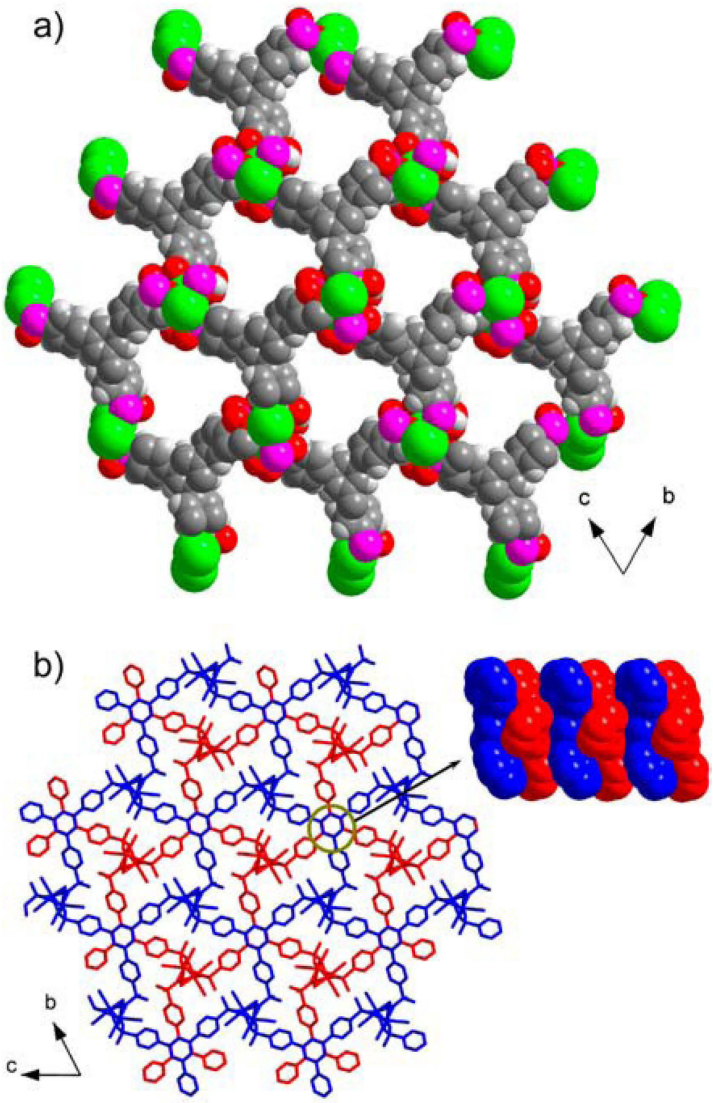

*Figure 4: X-ray structure of **2.** a) Space-filling model of a single non-interpenetrated layer showing the channels present along the a –axis (19.36 x 14.83 Å); b) Wireframe diagram showing the relation of the two interpenetrated nets. The inset is a space-filling diagram of the pi-stacking down the a-axis of the central arene ring of **PTAB** molecules.*

The stability of **2** was examined using thermogravimetric analysis. Compound **2** exhibits an initial two step weight loss (65-200°C, loss of five H_2O, 10.33% obs., 10.95% calc.; 200-400°C, loss of CH_3O, 3.21% obs., 3.78% calc.). Gas sorption of **2** using CO_2 indicated that it is microporous (Type 1 isotherm) with a BET surface area of 146 m^2/g (Figure 5). In a separate experiment, the reversible uptake of water vapour by **2** was examined over three heating/cooling

cycles from 25 to 150°C. Compound **2** takes up 14.14, 14.11 and 13.63 % in the successive cycles. (Figure 6) More interestingly, when **2** was left standing in air, IR spectra indicated it took up CO_2 from air. This unusual behaviour was investigated by heating **2** up to 100°C in dry N_2 on the TGA, to lose surface and bound water molecules, and then it was allowed to stand at RT under CO_2 for 2 hours. A 2% weight gain, corresponding to 0.4 moles of CO_2/FU, was observed. Over three sorption/desorption cycles in the temperature range of 25 to 300°C, a 2.5 - 3% CO_2 uptake was observed.

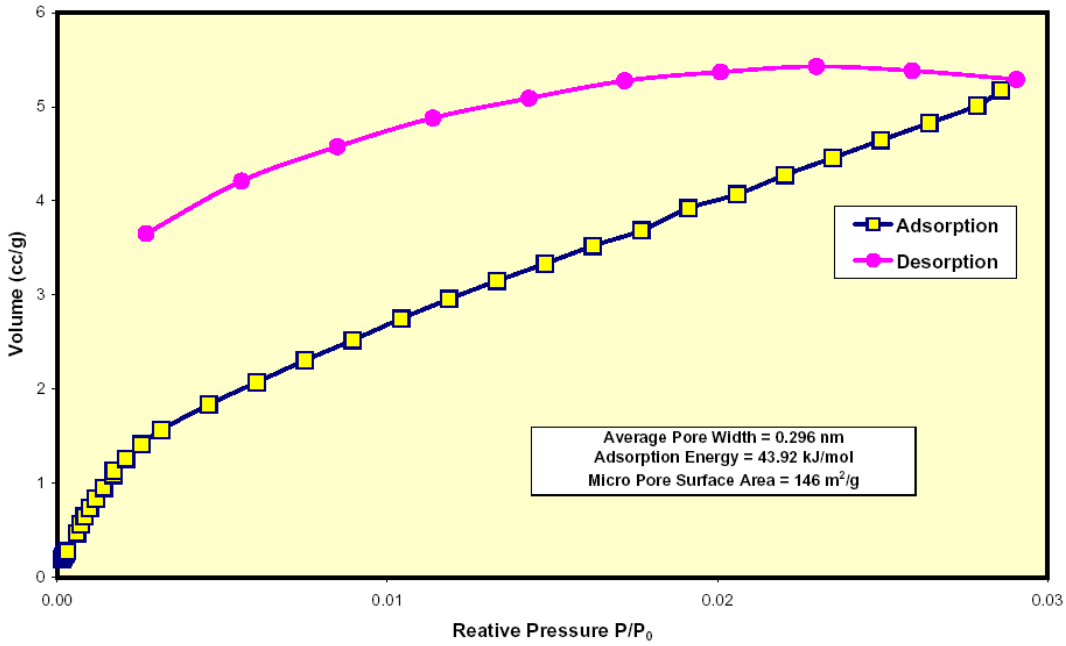

*Figure 5: CO_2 sorption analysis of **2**. Analyses were performed at Hiden Isochema on an IGA001 gravimetric sorption analyzer.*

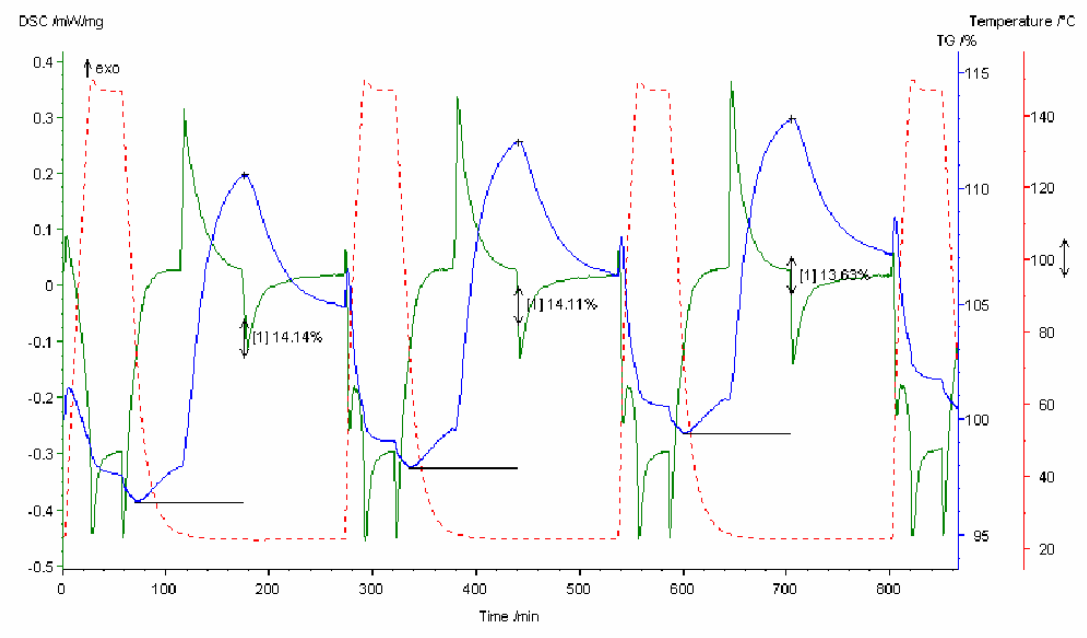

*Figure 6: Reversible water vapour uptake by **2** as monitored by TGA.*

Compound **2** presents several noteworthy features. The ligand **PTAB** was designed specifically to disfavour a densely packed solid and the rigid trigonal core directs the formation of an interpenetrated microporous structure. The framework is stabilized both by the 1-D inorganic columns and perfectly pi-stacked central aryl groups of **PTAB** molecules. While the 2-fold interpenetration diminishes the porosity, it is not a given that, in the absence of the aryl-aryl stacking that results from the interpenetration, the structure would be stable to collapse. Thus, it is difficult to say whether the inorganic column in **2** represents an "infinite secondary building unit"[12] or whether it is a compromised form to allow the pi-stacking. That said, the topology of **2** has design implications. The obvious means of increasing porosity would be to add additional phenyl spacers in **PTAB** off the core. With the structure of **2** being stabilized by the pi-stacking, lengthening the spacers in **PTAB** would not increase the likelihood of a more interpenetrated structure as with cubic or diamond networks. Thus, porosity should be greatly enhanced.

4 A New Linear Phosphonate Linker for MOFs

The ligand, 1,4-dihydroxy-2,5-benzenediphosphonic acid, H_4DHBP, was prepared with the intent of forming a chelating ring between the hydroxyl group and the phosphonate. With Zn^{2+} in DMF, a phase pure product, $Zn(H_2DHBP)(DMF)_2$, **3**, was formed with a structure of 1-D columns of phosphonate-bridged Zn centers. From these columns, the R groups protruded in four directions to form a square grid. The role of the non-coordinating hydroxyl groups was not to perturb the structure by chelation but rather simply by steric hindrance. To compare, 1,4-benzenediphosphonic acid readily forms layered structures with most metals.[16] Through PXRD

and TGA measurements, it was determined that the Zn complex was stable to loss of ~80% of the included DMF molecules, which inferred porosity. CO_2 and N_2 sorption analysis gave BET surface areas of 216m^2/g and 209m^2/g, respectively. Upon complete loss of DMF, a loss of order was observed by PXRD, but order was regained upon resolvation. The free hydroxyl group in this compound represented a potentially reactive site for post-synthetic modification.

4.1 Experimental

Synthesis of tetraethyl 1,4-phenylene bis(phosphate), PBP

A mixture of hydroquinone (22.0 g, 0.20 mol), carbon tetrachloride (180 mL), and diethyl phosphite (53.6 mL, 0.416 mol) was cooled to 0 ^oC, and then triethylamine (57.2 ml, 0.416 mol) was added dropwise. The mixture was stirred overnight at room temperature. The organic layer was washed with deionized water (4 x 200 mL) until it was clear. The organic fraction was concentrated on the rotary evaporator. Then the pale yellow syrup was dissolved in chloroform (300 mL) and dried over anhydrous Na_2SO_4 overnight. Filtration and removal of solvent on a rotary evaporator left tetraethyl 1,4-phenylene bis(phosphate), PBP, as a colorless liquid. Yield: 58.8g (0.154 mol), 77%. 'H NMR ($CDC1_3$/Me_4Si) δ(ppm): 1.30 (t, J = 7 Hz, 12 H, CH_3), 3.95-4.20 (m, 8 H, CH_2), 7.16 (s, 4 H, Ar); ^{13}C NMR ($CDC1_3$/Me_4Si) δ(ppm): 1 7.20 (s, $POCH_2CH_3$), 65.77 (s, $POCH_2CH_3$), 122.20 (s, C_2 C_3, C_5, C_6), 148.69 (s, C_1 and C_4); ^{31}P NMR δ(ppm): -6.35. Elemental analysis calculated for PBP is: C 43.99, H 6.33; found: C 43.90 H 6.09; FT-IR (cm^{-1}, KBr): υ(PO_3) 1160.52 cm^{-1} (w), 1104.24 cm^{-1} (m), 1031.00 cm^{-1} (s), 981.18 cm^{-1} (m), 938.759 cm^{-1} (m).

Synthesis of tetraethyl (2,5-dihydroxy-1,4-phenylene)bis(phosphonate) , DHPE

THF was dried by refluxing with Na for three days and diisopropylamine was refluxed with NaH for one hour before use. To a solution of diisopropylamine (22.4 g, 0.22mol) in THF (100 mL) at -78 ^oC under nitrogen was added n-butyllithium (136.6 ml, 1.6M in hexane, 0.217mol). The mixture was stirred for 30 min and PBP (19.0 g, 0.05mol) in THF (100 mL) was then added via syringe. The mixture was stirred at -78 ^oC for 1 h. The dry ice-acetone bath was then removed and the mixture was allowed to stir for an additional 1 h. The reaction was poured over a mixture of a saturated solution of ammonium chloride (150 mL) and ether (200 mL). The ether layer was separated and a white precipitate was collected. The aqueous layer was extracted with methylene chloride (3 x 150 mL). The combined organic extracts were dried over anhydrous Na_2SO_4. Filtration and removal of solvent on a rotary evaporator gave tetraethyl (2,5-dihydroxy-l,4-phenylene)bis(phosphonate), DHPE, as a pinkish solid. This was combined with the other precipitate, purified by double recrystallization from methylene chloride/petroleum ether and dried in a desiccator. White crystalline solid was collected. Yield: 14.2g (0.036 mol), 74.6%. m.p. 219-220 ^oC; 'H NMR ($CDC1_3$/Me_4Si) δ(ppm): 1.34 (t, J = 7 Hz, 12 H, CH_3) 4.16 (q, J = 7 Hz, 8H, CH_2), 7.00 (q, 2H, $^3J_{P\text{-}H}$ =8 Hz), 9.65 (s, 2H, OH); ^{13}C NMR ($CDC1_3$) δ(ppm): 17.3 (s, CH_3), 64.3 (s, CH_2), 117.6 (d, J=*177.7*Hz, C_1 and C_4); 120.5 (dd, $^2J_{P\text{-}C}$= 5.8 Hz and $^3J_{P\text{-}C}$ =18.5Hz, C3 and C6), 154.7 (dd, $^2J_{P\text{-}C}$ = 5.9 Hz, $^3J_{P\text{-}C}$ = 18.5; ^{31}P NMR δ(ppm): +19.37; Anal. Calcd for $C_{14}H_{24}O_8P_2$: C, 43.99; H, 6.33; Found: C, 43.38; H, 6.14. FT-IR (cm^{-1}, KBr): υ(PO_3) 1160.52 cm^{-1} (w), 1097.24 cm^{-1} (w), 1027.00 cm^{-1} (s), 957.18 cm^{-1} (s).

Synthesis of 2,5-dihydroxy-l,4-phenylene)bis(phosphonic acid), H_4DHBP

A mixture of DHPE (5.0 g, 12.9 mmol), 18% HC1 (50 mL), and dioxane (50 mL) was refluxed for 16 h. The solvents were removed on a rotary evaporator and the residue was refluxed with 18% HCl (50 mL) with 1g activated carbon for another 16 h. After filtration and solvent removal, a white solid, H_4DHBP, was collected. The solid H_4DHBP was then recrystallized with H_2O and methanol twice to yield colorless long needles. Yield: 1.1 g (4.07 mmol), 31.4%.; mp 219-220 ˚C; 'H NMR δ(ppm):7.10 (d, d $^3J_{P-H}$ = 6Hz, $^4J_{P-H}$ = 7Hz*);* ^{31}P NMR (D_2O) + 12.94; ^{13}C NMR. (D_2O), ^{13}C NMR (D_2O) δ (ppm):15.6951 (s, CH_3), 61.71 (s, CH_2), 118.9 (d, *J=177.7*Hz, C_1 and C_4); 120.5 (d d, ^2Jp-c= 5.8 Hz and ^3Jp-c=18.5Hz, C3 and C6), 150.7 (d d, ^2Jp-c= 5.9 Hz, ^3Jp-c = 18.5; Anal. Calcd for $C_6H_8O_8P_2$: C, 26.68; H, 2.99. Found: C, 27.43, H, 3.38.

Synthesis of $\{[Zn(H_2DHBP)](DMF)_2\}_\infty$, 3

Bulk phase synthesis: H_4DHBP (0.108 g, 0.400 mmol) was dissolved in H_2O (10 mL) and added to a solution of $Zn(ClO_4)_2$ (0.0744 mg, 0.20 mmol) in H_2O (5 mL). Tetraethylammonium hydroxide (35 wt % aq., 5 drops) was added to adjust the pH of the solution to 2. The mixture was then refluxed while slowly adding DMF (5 mL) dropwise until a bulk precipitate was formed and collected. Yield: 44 mg (0.088mmol), 22%.

Crystal growth: To a solution of H_4DHBP (54mg, 0.20 mmol) in H_2O (2.5 mL) was added a solution of $Zn(ClO_4)_2$ (37.2mg, 0.10 mol) in H_2O (2.5 mL). Tetraethylammonium hydroxide (35 wt % aq) was used to adjust the pH to 2.5. The mixture was then filtered and DMF (10 mL) was allowed to diffuse slowly into the solution. Colorless brick like crystals formed in two days later. Yield: 10 mg (0.002 mol), 10%. Anal. Calcd for $\{[Zn(H_2DHBP)](DMF)_2\}_\infty$: C, 30.05; H, 4.20; N, 5.84; Found: C, 29.59; H, 4.14; N, 4.80. FT-IR (cm^{-1}, KBr): υ(PO_3) 1200.00 cm^{-1}, 1117.39 cm^{-1}, 1000.00cm^{-1}, 934.78 cm^{-1}.

Crystal growth of $\{[Zn(H_2DHBP)](Py)_2(MeOH)_2\}_\infty$, 3

$[ZnCO_3]_2{\cdot}[Zn(OH)_2]_3$ (22 mg, 0.04 mmol) was added to a solution of H_4DHBP (54mg, 0.20 mmol) in H_2O (5 mL). The mixture was then stirred for 30 minutes. A white solid was filtered, and then dissolved in HCl (0.5 M, 4.0 mL). Pyridine (0.5 mL) and Methanol (4 mL) was allowed to diffuse slowly into the solution. Several colorless brick like crystals formed in three days later with very low yield. Unit cell: Space group: P-1; a = 10.2480 (3) Å, b = 12.0870(3) Å, c = 14.8320(3) Å; α= 76.801(2)^o, β= 79.238(2),λ= 71.856(2); Z = 4; V = 1686.4(1) Å.

4.2 Results and Discussion

The ligand, 1,4,-dihydroxy-2,5-benzenediphosphonic acid (H_4DHBP), was prepared in three steps from hydroquinone.[17] Compound **3** was prepared, both in bulk form and as single crystals, from $Zn(ClO_4)_2$ and H_4DHBP as a DMF solvate. Compound **3** contains DHBP as a tetra-anionic ligand. The asymmetric unit of **3** contains only one Zn^{2+} ion and half a DHBP molecule. Building up the structure of **3**, tetrahedral Zn^{2+} centers are coordinated by four oxygen atoms from four different phosphonate groups from four different DHBP molecules (Zn-O2 = 1.936(2) Å, Zn-O3 = 1.918(2) Å). Only two oxygen atoms of each RPO_3^{2-} group coordinate to Zn. This primary coordination forms 1-D chains of RPO_3-bridged Zn ions along the *c*-direction (Figure 7a). Zn centers repeat at 4.630(1) Å in the chain. Although grown from an aqueous solution, no

water is coordinated to the Zn centers. The OH groups of DHBP are protonated and uncoordinated. The phenyl groups of the four DHBP molecules ligated to each Zn center form two mutually orthogonal pairs. This serves to crosslink the 1-D columns along *c* in both the *a* and *b* directions and results in the 3-D porous structure shown in Figures 7b and 7c. The pores in **3** measure 10.46(1) Å x 10.46(1) Å between phenyl groups and 14.01(1) Å between Zn atoms. The pores are filled with included DMF molecules. Viewed along the diagonals between the *a* and *b* axes, owing to the orientation of the phenyl rings, the pores orthogonal to the *c*-axis are smaller with a narrow point of 4.37(1) Å (Figure 7).

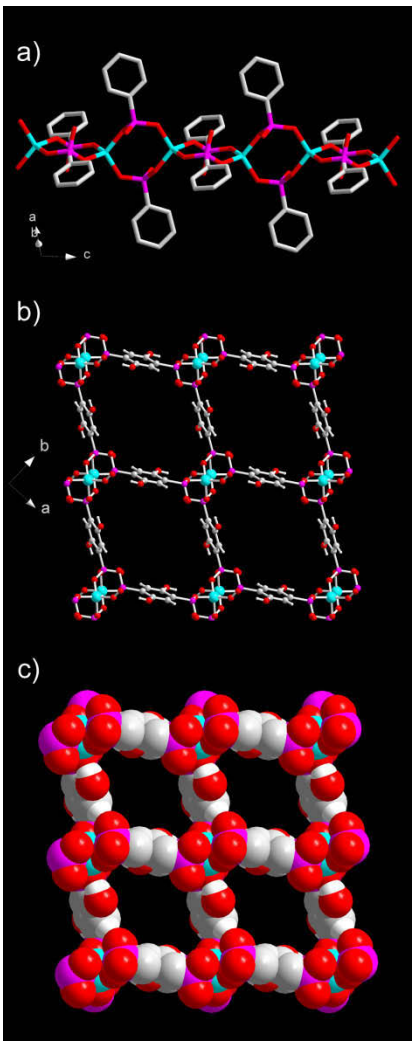

Figure 7: Single crystal X-ray structure of ***3****. (a) View of a single RPO_3-bridged Zn chain running down the c-axis. (b) View looking down the c-axis showing the network of pores. (c) A space-filling depiction of the porous network*

PXRD analysis of a precipitate of **3** confirmed that it can be generated as a bulk material (Figure 8). Thermogravimetric analysis and PXRD showed that **3** was stable to the loss of 80 % of included DMF molecules. The stability to the loss of guests inferred porosity and so gas sorption

analysis was performed on **3**.[14] CO_2 and N_2 sorption isotherms confirmed permanent pores. A Type 1 isotherm, with considerable hysteresis, was observed for CO_2 (see supporting) giving a Brunauer-Emmett-Teller (BET) surface area of 216 m^2/g.[14] With N_2, a Type I isotherm was observed (Figure 7) giving a BET surface areas of 209 m^2/g. Upon loss of all the DMF, loss of order is seen in the PXRD.

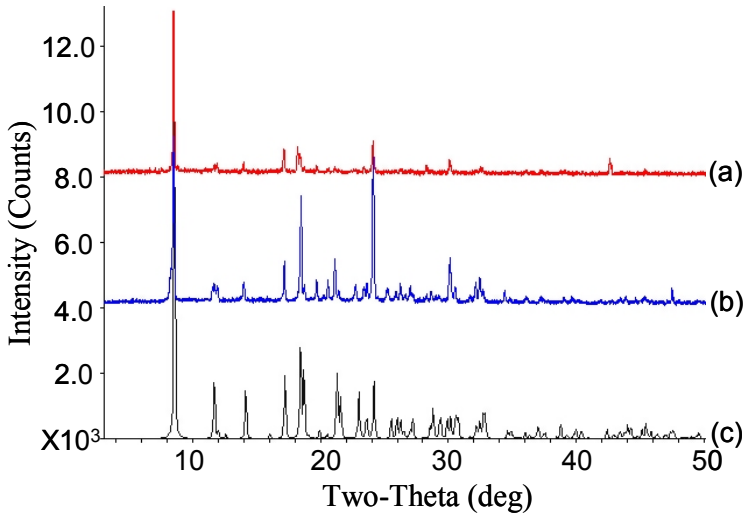

*Figure 8: PXRD of **3**. (a) After heating to 200 °C, (b) as a bulk precipitate, (c) simulated from the single crystal structure.*

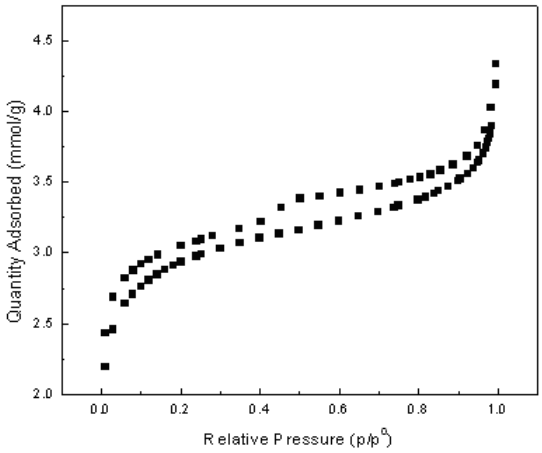

*Figure 9: Sorption isotherm of **3** at 77K. Sorption is the lower curve and desorption the upper curve.*

Multiple strategies to generate pores in crystalline metal phosphonate materials have been pursued. Attempts to intersperse phosphate as a spacer between pillaring diphosphonates in layered solids result in pores but with an undesirably high size dispersity.[18] Examples of porous metal methylphosphonates have been reported.[19] The metal phosphonate groups in these systems

assemble into hexagonal networks driven by the inefficient packing of methyl groups in a simple layered arrangement. More generally, the organic spacer can be chosen so as to preclude formation of a dense material. This often leads to solids with lower degrees of order although not always. Use of phosphonated metalloligands has also been explored where again, retention of crystallinity is challenging but not impossible.[20] The most common route to porous metal phosphonates involves adding a secondary ligating group in proximity to the RPO_3^{2-} to direct the metal ligand assembly away from a simple layered motif.[21] These solids though are generally not homoleptic phosphonates.

In this light, compound **3** is quite unusual. The modification to the simple phenyl diphosphonate skeleton, which readily forms a dense layered motif, is relatively minor compared to other ligands which have been prepared.[8-10,21] Moreover, the hydroxyl groups on L do not coordinate to the Zn centers and play exclusively a steric role. Yet, obviously, the addition of the two hydroxyl groups perturbs the packing sufficiently to disfavour formation of a layered motif and generate a regular open structure. Packing of any solid can be viewed as a balance of favourable interactions between metals and coordinating atoms and also maximizing non-covalent interactions. The open framework in **3** is sustained exclusively by 1-D chains of phosphonate-bridged Zn ions; no interactions exist between DHBP molecules. Yaghi et al. have discussed the packing of rods as "infinite secondary building units (SBU's),"[22] with respect to the range of 1-D chain structures observed with carboxylate ligands. The stability of such linkers would be expected to be enhanced by having metal ions in as close to ideal geometries as possible as well as having low degrees of coordinated solvent. Looking at the 1-D Zn chains in **1**, the Zn ion has a slightly distorted tetrahedral geometry ($\angle$ O-Zn-O = 104.7(1) – 118.9(1)$^\circ$). The coordination sphere of Zn is composed solely of strongly ligated phosphonate oxygen atoms, no solvent is coordinated. As evidenced by the permanent porosity, clearly this is a very robust skeleton. As only two oxygen atoms from each phosphonate group coordinate, each RPO_3^{2-} unit can be considered as functioning like a "charge-assisted carboxylate" in the formation of the robust infinite SBU. Several clusters and aggregates have been observed for Zn phosphonates,[23] largely dictated by the sterics of the R group, however, nothing so regular as to merit the SBU designator has been observed. The generality of whether an *ortho*-situated hydroxyl group in other aryl phosphonates results in the same SBU as observed in **1**, and hence other (more) porous metal phosphonates, is under study. A final point of interest is that the uncoordinated hydroxyl group in **1** represents a reactive site in the pores and a means to tune the chemical nature of the channels.

5 Copper and Zinc Complexes of (1,4-diphosphonobenzenebis(monoalkyl)esters)

In parallel to the approach shown in section 4 where an additional functional group was employed to broaden the organic linker and disfavour a densely packed structure, the use of a phosphonate mono ester was attempted to also form open structures. The ligand could be obtained by partial hydrolysis of the parent phosphonate diester in a controlled manner. Three compounds have resulted in new microporous solids, showing that the ligating ability is sufficiently strong to sustain permanent porosity.

5.1 Experimental

Synthesis of 1,4-benzenediphosphonatebis(dimethylester). (BDPDM)

1,4-dibromo benzene 9.44 g (40 mmol) and NiCl2 anhydrous 4.34 g (20 mmol) was placed into a two neck round bottom flask and then dried under vacuum while heating for 20 minutes. 1,3-diisopropylbezene (100 ml) was added after removing the vacuum. The flask was then fitted with a condenser and a dropping funnel. $P(OMe)_3$ (37.8 ml, 320mmol) was placed into the dropping funnel with 1,3-diisopropylbezene (30 ml). The solution was brought to reflux and the $P(OMe)_3$ solution was added slowly over 10 hours, followed by refluxing for 48 hours under argon. Then yellow components were distilled off under vacuum at 30 ^oC to obtain a brown solid residue. The solid was first washed with hexanes (100 mL) and then dissolved in diethyl ether. The yellow solution was taken to dryness after filtration and pale yellow solid was collected. Chromatography of the residue was performed on a column of silica gel using ethyl estate-methanol-acetic acid (100:5:1) as eluent. Rf :0.33. Yield: 8.47g (28.8 mmol), 72%. Anal. Calcd for BDPDM: C, 40.83; H, 5.48. Found: C, 40.77; H, 5.36; 1H NMR (400 MHz CDC13/Me4Si) δ (ppm): 3.77-3.81 (d, J = 11.1Hz, 12H, CH3); 7.87-7.92 (dd, 3JP-H=6.7, 4JP-H =10.4 Hz, 4H); 31P NMR (400 MHz CDC13/Me4Si) δ (ppm): 17.60; 13C NMR (100 MHz CDC13/Me4Si) δ (ppm): 50.22(d, CH3), 73.97-74.82 (t , C1 and C4), 128.15-130.04 (C2, C3, C5, C6). FT-IR (cm-1, KBr): 3442.07(vs), 3080.07(w), 3003.69(m), 2957.20(s), 2897.42(w), 2854.24(m), 2359.41(w), 2339.48(w), 1967.53(w), 1861.25(w), 1459.41(m), 1373.06(m), 1273.43(s), 1246.86(s), 1177.12(s), 1143.91(m), 1100.74(m), 1021.03(s), 861.62(m), 828.41(s), 771.96(s), 609.23(s), 552.77(s), 453.14(w), 419.93(m), 416.61(s).

Synthesis of Sodium benzene l,4- bis(phosphonate mono methyl ester (Na_2BDPMM)

A mixture of 1,4-benzenediphosphonatebis(dimethylester) (BDPDM) (5.0 g, 16.9 mmol), concentrated ammonia solution (20 mL), and methanol (10 mL) was refluxed for 16 h. The solvents were removed on a rotary evaporator and the white solid was collected. The white solid was dissolved with 5 ml distilled water and then passed down a 50W-X8 cation exchange column (Na^+ form) using distilled water as eluent. The clear solution was collected and the solution was taken to dryness on a rotary evaporator. A white solid, Na_2BDPMM was then collected. The solid Na_2BDPMM was then recrystallized twice from an H_2O/methanol mixture to yield white crystalline solid. Yield: 4.36 g (14.03 mmol), 83%. Anal. Calcd for Na_2BDPMM: C, 30.99; H, 3.25. Found: C, 30.90; H, 3.34; ^{1}H NMR (400 MHz D_2O) δ (ppm): 3.31-3.34 (d, *J* = 10.8Hz, 6H,CH_3), 7.54-7.81 (m, 4H). ^{31}P NMR (400 MHz D_2O) δ (ppm): 16.98; ^{13}C NMR (100 MHz $CDC1_3$/Me_4Si) δ (ppm): 51.85 (s, CH_3), 130.71-130.94 (d d, ^{2}Jp-c= 11.5 Hz, ^{3}Jp-c = 11.5, C_2, C_3, C_5, C_6), 134.32-136.07 (d, J_{P-C} = 175.0 Hz, C_1, C_4), FT-IR (cm^{-1}, KBr): 3425.46(vs), 2937.27(m), 2840.96(m), 2366.05(w), 2339.48(w), 1940.69(w), 1459.41(w), 1446.13(m), 1386.35(m), 1270.11(m), 1233.58(s), 1190.41(w), 1157.20(s), 1057.56(s), 1014.39(s), 821.77(m), 755.35(s), 592.62(s), 559.41(m), 489.67(m), 406.64(m).

Synthesis of Copper benzene l,4- bis(phosphonate mono methyl ester [CuBDPMM(H_2O)]$_\infty$, 4

$CuCl_2$ $2H_2O$ (17.1 mg, 0.10 mmol) was dissolved in deionized water (2.0 mL) and Na_2BDPMM (31.1 mg 0.10 mmol) was dissolved in deionized water (2.0 mL), separately. The two solutions were then mixed in a 10 mL glass vial and the resulting mixture was dispersed by sonication for 5 minutes and MeOH (10 mL) was allowed to diffuse slowly into the solution. Blue brick like crystals formed in ten days. Yield: 10 mg (0.002 mol), 10%. Anal. Calcd for [CuBDPMM(H_2O)]$_\infty$: C, 27.80; H, 3.50;; Found: C, 27.26; H, 3.52; DSC/TGA: 25 ºC–98 ºC, -5.00% (119.7 J g^{-1}, exo)obsd and -5.21% calcd for loss of 1.0 H_2O, 375ºC–450 ºC . -18% (106.3 J g^{-1}, endo) FT-IR (cm^{-1}, KBr): 3500(vs), 2943.91(w), 2837.64(w), 2366.05(s), 2322.88(w), 1977.49(w), 1442.80(w), 1456.09(w), 1389.67(w), 1187.08(s), 1163.84(s), 1070.85(s), 861.62(w), 795.20(s),599.26(s), 569.37(m), 512.92(w), 433.21(w).

The Zn complex of the monoethylester derivative, **5**, was prepared analogously (employing $P(OEt)_3$ in the first step of the synthesis, see Figure 10). Small amounts of single crystals were obtained however, at this time bulk phase pure samples are in preparation. The crystals were able to be analyzed to obtain preliminary structures.

5.2 Results and Discussion

The new ligands BDPMM and BDPME, methyl and ethyl phosphonate monoesters of 1,4-substituted benzenes, respectively, were prepared and isolated as their Na salts. The overall synthetic scheme is given in Figure 10.

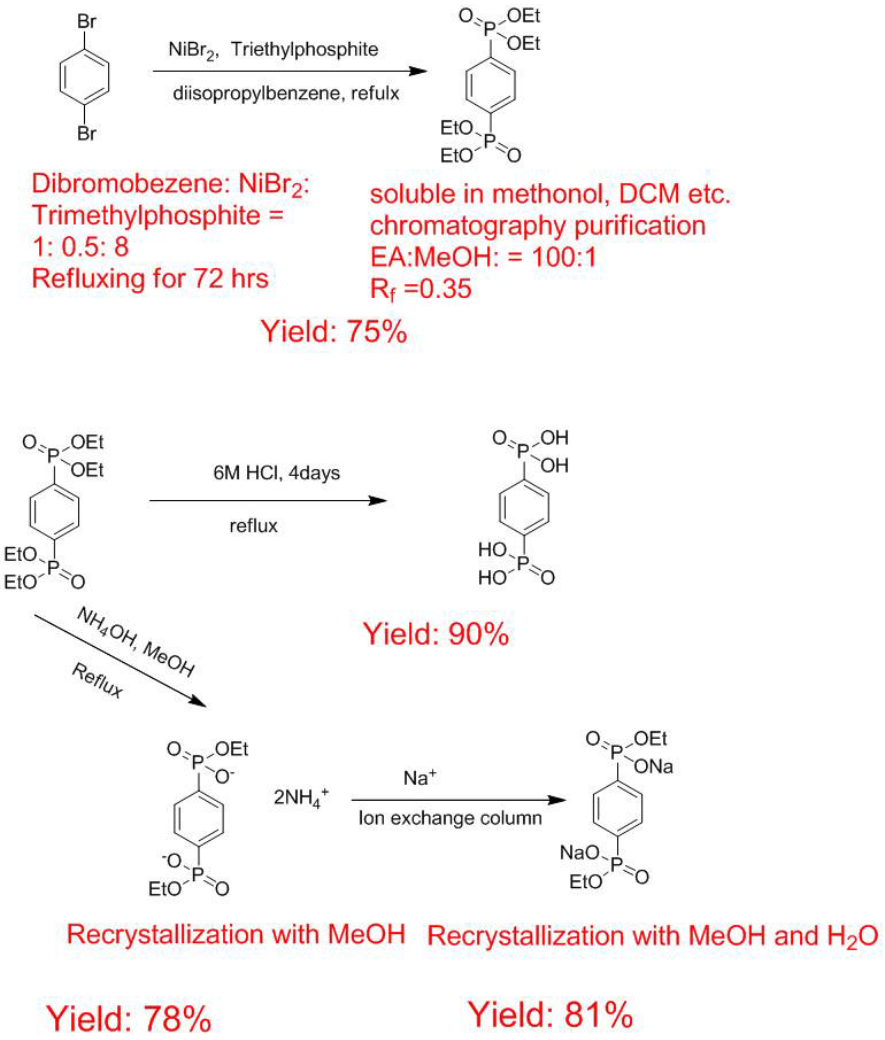

Figure 10: Synthetic scheme for monomethyl and monoethylesters of 1,4-benzenediphosphonic acid.

The phosphonate monoesters are monoanionic in comparison to the the dianionic phosphonates and also possess an alkyl group as a variable tether which could be used to further regulate pore size. The fundamental hypothesis in the design of the structures was that removing the ligating ability of one of the three oxygen atoms on the P atom would make the formation of a dense hybrid inorganic organic structure impossible. This was borne out by the crystal structures of the Cu(II) complex of the methyl ester, **4**, and the Zn(II) complex of the ethyl ester, **5**, and their respective gas sorption isotherms.

The structures of **4** can be described as 1-D columns of Cu(II) ions doubly bridged by two O atoms of two different BDPMM ligands into square nets. The rhomboidal pores of the nets, excluding vdW radii measure 7.0 x 15.7 Å. The structure is quite similar to that of compound **3** on a macroscopic level. The pores are only 1-D so, while the structure is more likely to be robust,

the diffusion of gases into the pore is more restricted. Figure 11 shows the structure of 4 showing the pores. Notably the alkyl groups of the alkyl esters protrude directly into the pores.

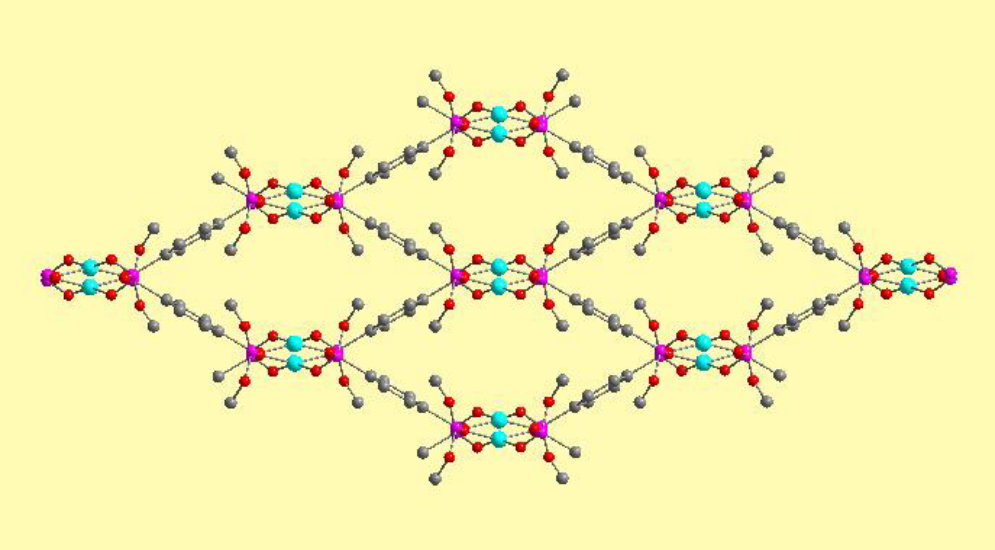

*Figure 11: Structure of **4**, the Cu(II) complex of the monomethylester of 1,4-benzenediphosphonic acid.*

The structure of compound **5** was significantly different from **4** (and **3**). A common feature was that the Zn(II) ions were bridged into 1-D chains by the O atoms of the phosphonate esters. However, rather than the phenylene spacers linking the structure into a square grid, a corrugated layer structure was observed. These layers lay roughly in the ac plane with the ethyl groups of the phosphonate esters projecting away from the layers. Normally, the fact that a layered motif is observed would mean a dense structure, however, unusually, the alkyl groups associate via vdW interactions and appear to pillar the layers (Figure 12) resulting in pores (9.2 x 11.5 Å excluding vdW radii). Powder X-ray diffraction showed that the structure of **5** was retained after removal of volatiles. This was again, a surprising result as that would imply that the vdW interaction between alkyl pillars (interalkyl contacts range from 4.0-4.4 Å) was sufficient to sustain a pore in the solid.

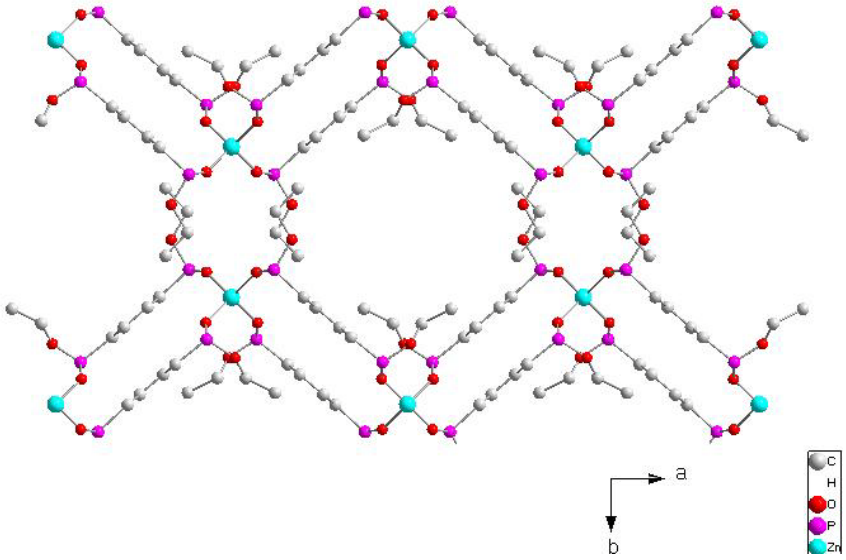

Figure 12: Structure of the Zn(II) complex of the monoethylester of 1,4-benzenediphosphonic acid. Layers lie in the ac plane (l-r in the picture) and the pores run along the c-axis.

CO_2 sorption was performed at 273K to probe the porosity of both **4** and **5**. In the case of **4**, porosity was expected and a Type I gas sorption isotherm was observed (Figure 13). The surface area extracted from this isotherm by fitting to a DFT model was 170 m^2/g. This is a modest value but, from the perspective of design of sorbents, quite promising as it confirmed the pore structure was stable to evacuation. Pore size could be expanded by using longer linkers as often demonstrated with MOF chemistry. Moreover, the particular topology shown by **4** would not interpenetrate with longer linkers. On a less positive note, the structure likely would not shift away from 1-D pores.

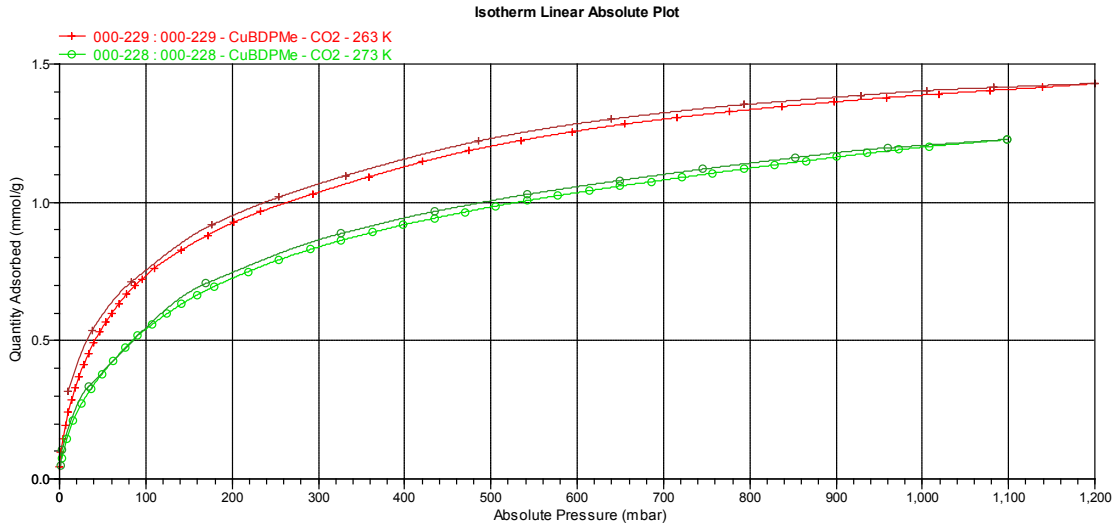

*Figure 13: CO_2 sorption isotherm for compound **4** at 263 (upper) and 273K.*

Intuitively, there was little optimism for the observation of permanent porosity from the non-covalently pillared layered structure observed for **5**, however, CO_2 sorption analysis corroborated the powder X-ray diffraction experiment and showed that, indeed, pores accessible to external gases were present. The CO_2 sorption isotherm (Figure 14) for **5** is also a Type I isotherm and a DFT fit of the surface area gave a value of 150 m^2/g.

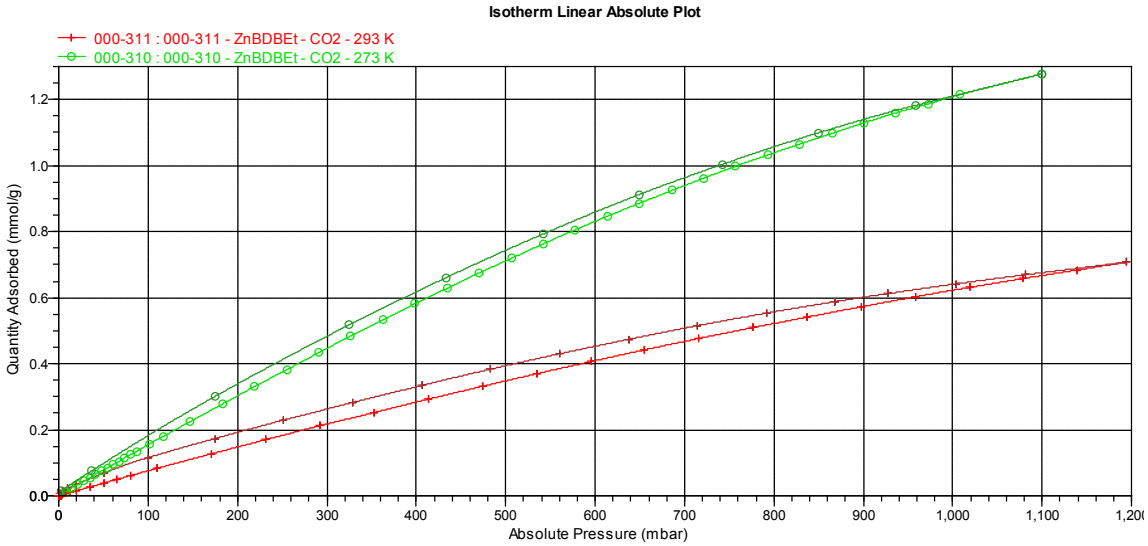

*Figure 14: CO_2 sorption isotherm for compound **5** at 263 (upper) and 273K.*

The actual uptake in **5** is not so abrupt as in **4** (or the other MOFs reported here). This is interesting in that the layers in **5** could further separate (swell) with increased pressure of guest molecules. Often layered materials will demonstrate guest inclusion after some critical pathway for ingress between the layers has been activated, perhaps by a smaller guest molecule. In this

case, the material appears pre-activated and increased sorption at higher pressures may be potentially observed. Figure 15 shows a space-filling representation of the pores in **5**. Prior to the gas sorption analyses, our perception would have been that this depiction was artificial (as we anticipated pore collapse). However, it appears this representation is a minimal one of the potential porosity of compound **5**. Presently, we do not have access to a higher pressure sorption apparatus but such experiments will be studied in the future.

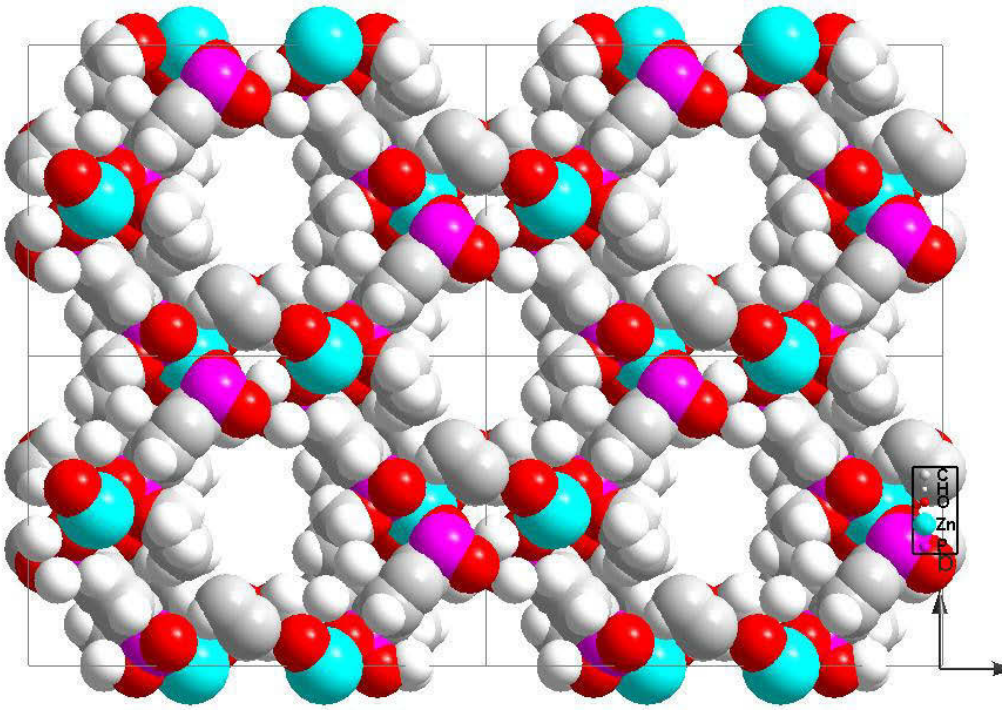

Figure 15: Space-filling representation of the pores in compound **5**.

6 Conclusion

Four different organic spacer units were prepared and frameworks studied with different metal ions under different preparative conditions. With each new linker multiple new porous materials were obtained, at least one of which was characterized by X-ray crystallography to give precise molecular dimensions of the pores. Pores were observed in the X-ray structure but definitive proof came in the form of gas sorption measurements showing surface areas in the rages of 100-500 m^2/g. Pores were probed with N_2 gas at 77K and CO_2 at either 273 or 293K. All new compounds were thoroughly characterized. Details of the specific compounds are provided in the report.

Table 1. *Comparison of MOF Properties*

COMPOUND	CO_2 SURFACE AREA (m^2/g)	COMMENTS
$Cu_3H_3ADTP(OH)\cdot 3H_2O$	*200*	*2800m^2/g predicted for N_2 absorption by modelling for desolvated MOF*
SrPTAB	*146*	
$Zn(H_2DHBP)(DMF)_2$	*216* (209 N_2)	Stable to loss of up to 80% of DMF, loss of all DMF results in disordered phase, order is regained on resolvation
$CuBDPMM(H_2O)$	*170*	
$ZnBDPMM(H_2O)$	*150*	

References

[1] G. Alberti, U. Costantino, S. Allulli and N. Tomassini, *J. Inorg. Nucl. Chem.*, 1978, **40,** 113.

[2] A. Clearfield, *Prog. Inorg. Chem*. 1998, **47**, 371.

[3] G. Alberti; U. Costantino, in *Comprehensive Supramolecular Chemistry*, Vol. 7; (Eds. J. L. Atwood, J. E. D. Davies, D. D. MacNicol, F. Vögtle), Elsevier Science, New York, 1996.

[4] K. Maeda, *Micropor. Mesopor. Mater*. 2004, **73**, 47.

[5] G. Alberti, R. Vivani, F. Marmottini and P. Zappelli, *J. Porous Mater*. 1998, **5**, 205.

[6] M. B. Dines, R. E. Cooksey, P. C. Griffith and R. H. Lane, *Inorg. Chem.* 1983, **22** 1003.

[7] G. Alberti, U. Constantino, F. Marmottini, R. Vivani and P. Zappelli, *Angew. Chem. Int. Ed. Engl.* 1993, **32**, 1357.

[8] M. V. Vasylyev, E. J. Wachtel, R. Popovitz-Biro, R. Neumann, *Chem. Eur. J.* 2006, **12**, 3507.

[9] M. Vasylyev, R. Neumann, *Chem. Mater.* 2006, **18**, 2781.

[10] J. M. Taylor, A. M. Mahmoudkhani, G. K. H. Shimizu, *Angew. Chem. Int. Ed.* 2007, **46**, 795.

[11] N. L. Rosi, M. Eddaoudi, J. Kim, M. O'Keeffe, O. M. Yaghi, *CrystEngComm* 2002, **2**, 401.

[12] B. L. Chen, M. Eddaoudi, S. T. Hyde, M. O'Keeffe, O. M. Yaghi**,** *Science* 2002, **295**, 469.

[13] R. Vaidhyanathan, A, H. Mahmoudkhani and G. K. H. Shimizu, *Can. J. Chem.,* 2009, **87**, 247.

[14] E. Weber, et al., *J. Chem. Soc. Perkin Trans. II*, 1988, 1251.

[15] M. Mar Gomez-Alcantara, et al., *Inorg. Chem.* 2004, **43**, 5283-5293

[16] S. Konar, J. Zon, A. V. Prosvirin, K. R. Dunbar and A. Clearfield, *Inorg. Chem.* 2007, **26**, 5229.

[17] B. Dhawan, D. Rehmore, *J. Org. Chem*. 1984, **49,** 4018.

[18] N. J. Clayden, *J. Chem. Soc. Dalton Trans*. 1987, 1877.

[19] K. Maeda, J. Akimoto, Y. Kiyozumi, F. Mizukami, *Angew. Chem. Int. Edn.* 1994*,* **33,** 2335.

[20] C.D. Wu, A. Hu, L. Zhang, W. Lin, *J. Am. Chem. Soc.* 2005*,* **127**, 8940.

[21] Evans, O. R.; Ngo, H. L.; Lin,W. *J. Am. Chem. Soc.* 2001, **123**, 10395.

[22] N. L. Rosi, J. Kim, M. Eddaoudi, B. Chen, M. O'Keeffe. O.M. Yaghi, *J. Am. Chem. Soc*. 2005, **127**, 1504.

[23] M. I. Khan, J. Zubieta, *Prog. Inorg. Chem*. **1995**, *43*, 1.

List of symbols/abbreviations/acronyms/initialisms

DND	Department of National Defence
DRDC	Defence Research & Development Canada
DRDKIM	Director Research and Development Knowledge and Information Management
DSC	Differential Scanning Calorimetry
MOFs	Metal Organic Frameworks
PXRD	Powder X-ray Difraction
R&D	Research & Development
TGA	Thermogravimetric Analysis

This page intentionally left blank.

Distribution list

Document No.: DRDC Atlantic CR 2010-201

LIST PART 1: Internal Distribution by Centre

3 DRDC Atlantic Library (1 hard copy, 2 CDs)

1 Dr Paul Saville, DRDC Atlantic

4 TOTAL LIST PART 1

LIST PART 2: External Distribution by DRDKIM

1 Library and Archives Canada, Attn: Military Archivist, Government Records Branch

1 Dr George Shimizu, Department of Chemistry, University of Calgary, Calgary, AB T2N 1N4

1 Dr Scott Duncan, DRDC Suffield

1 DRDKIM

4 TOTAL LIST PART 2

8 TOTAL COPIES REQUIRED

This page intentionally left blank.

DOCUMENT CONTROL DATA

(Security classification of title, body of abstract and indexing annotation must be entered when the overall document is classified)

1. ORIGINATOR (The name and address of the organization preparing the document. Organizations for whom the document was prepared, e.g. Centre sponsoring a contractor's report, or tasking agency, are entered in section 8.)

Dr Geroge Shimizu
Department of Chemistry
University of Calgary

2. SECURITY CLASSIFICATION (Overall security classification of the document including special warning terms if applicable.)

UNCLASSIFIED

3. TITLE (The complete document title as indicated on the title page. Its classification should be indicated by the appropriate abbreviation (S, C or U) in parentheses after the title.)

Modelling Assisted Design And Synthesis Of Highly Porous Materials For Chemical Adsorbents

4. AUTHORS (last name, followed by initials – ranks, titles, etc. not to be used)

Shimizu, G.

5. DATE OF PUBLICATION (Month and year of publication of document.)

October 2010

6a. NO. OF PAGES (Total containing information, including Annexes, Appendices, etc.)

46

6b. NO. OF REFS (Total cited in document.)

24

7. DESCRIPTIVE NOTES (The category of the document, e.g. technical report, technical note or memorandum. If appropriate, enter the type of report, e.g. interim, progress, summary, annual or final. Give the inclusive dates when a specific reporting period is covered.)

Contract Report

8. SPONSORING ACTIVITY (The name of the department project office or laboratory sponsoring the research and development – include address.)

Defence R&D Canada – Atlantic
9 Grove Street
P.O. Box 1012
Dartmouth, Nova Scotia B2Y 3Z7

9a. PROJECT OR GRANT NO. (If appropriate, the applicable research and development project or grant number under which the document was written. Please specify whether project or grant.)

9b. CONTRACT NO. (If appropriate, the applicable number under which the document was written.)

W7707-042697

10a. ORIGINATOR'S DOCUMENT NUMBER (The official document number by which the document is identified by the originating activity. This number must be unique to this document.)

10b. OTHER DOCUMENT NO(s). (Any other numbers which may be assigned this document either by the originator or by the sponsor.)

DRDC Atlantic CR 2010-201

11. DOCUMENT AVAILABILITY (Any limitations on further dissemination of the document, other than those imposed by security classification.)

Unlimited

12. DOCUMENT ANNOUNCEMENT (Any limitation to the bibliographic announcement of this document. This will normally correspond to the Document Availability (11). However, where further distribution (beyond the audience specified in (11) is possible, a wider announcement audience may be selected.))

Unlimited

13. ABSTRACT (A brief and factual summary of the document. It may also appear elsewhere in the body of the document itself. It is highly desirable that the abstract of classified documents be unclassified. Each paragraph of the abstract shall begin with an indication of the security classification of the information in the paragraph (unless the document itself is unclassified) represented as (S), (C), (R), or (U). It is not necessary to include here abstracts in both official languages unless the text is bilingual.)

A new family of metal organic framework materials was studied which relied on organophosphonate molecules as organic linkers between metal ion aggregates as connecting nodes. These materials could form new porous sorbents with the ability to tune the pore size, pore shape and the nature of the chemical functionalities lining the pores. Linear, trigonal and tetrahedral polyphosphonate molecules were studied as well as functionalized linear linkers, all of which were successful in producing new porous solids. Additionally, the use of a linear phosphonate mono ester as a linker was studied, the first use of such a compound in a metal organic framework. New organic linkers were characterized by ^{1}H, ^{13}C and ^{31}P NMR spectroscopy as well as IR spectroscopy and elemental analyses. New network solids were characterized by powder and, when possible, single crystal X-ray diffraction as well as thermogravimetric analysis and gas sorption analyses. Several new families of new porous materials were developed which show promise for sorption of gaseous analytes.

Une nouvelle famille de réseaux métallo-organiques a été étudiée et dans laquelle des molécules d'organophosphonate constituent des liens organiques entre les agrégats d'ions métalliques faisant office de noeuds connecteurs. Ces matériaux pourraient former de nouveaux adsorbants poreux offrant la possibilité d'ajuster la taille et la forme des pores, et la nature des fonctionnalités chimiques à la surface des pores. Des molécules de polyphosphonate linéaires, trigonales et tétraédriques ont été étudiées, ainsi que des liens linéaires fonctionnalisés, et toutes ces molécules ont permis de produire de nouveaux solides poreux. En outre, l'utilisation d'un monoester de phosphonate linéaire comme lien a été étudiée, et il s'agissait de la première utilisation d'un tel composé dans un réseau métallo-organique. Les nouveaux liens ont été caractérisés par spectroscopie RMN ^{1}H, ^{13}C et ^{31}P, par spectroscopie infrarouge et par analyse élémentaire. Les nouveaux solides à structure de réseau ont été caractérisés par diffraction de poudre et, si possible, par diffraction des rayons X par cristal unique, analyse thermogravimétrique et analyse d'adsorption de gaz. Plusieurs nouvelles familles de nouveaux matériaux poreux ont été mises au point, et elles sont prometteuses pour la sorption des substances gazeuses à analyser.

14. KEYWORDS, DESCRIPTORS or IDENTIFIERS (Technically meaningful terms or short phrases that characterize a document and could be helpful in cataloguing the document. They should be selected so that no security classification is required. Identifiers, such as equipment model designation, trade name, military project code name, geographic location may also be included. If possible keywords should be selected from a published thesaurus, e.g. Thesaurus of Engineering and Scientific Terms (TEST) and that thesaurus identified. If it is not possible to select indexing terms which are Unclassified, the classification of each should be indicated as with the title.)

Porous Material; Organometallic Framework

This page intentionally left blank.

Defence R&D Canada

Canada's leader in defence
and National Security
Science and Technology

R & D pour la défense Canada

Chef de file au Canada en matière
de science et de technologie pour
la défense et la sécurité nationale

DEFENCE DÉFENSE

www.drdc-rddc.gc.ca